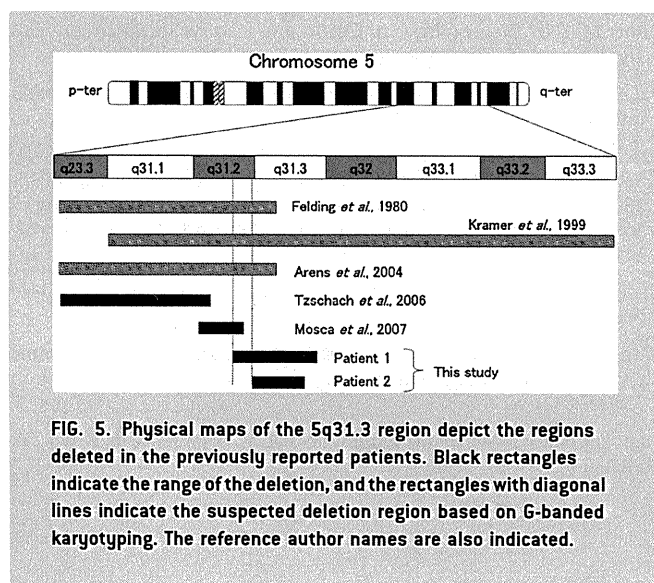


are sequentially organized on the 5q31.3 region (Fig. 3) [Yagi, 2008]. The other non-clustered PCDHs, *PCDH1* and *PCDH12*, were also included in this region. PCDHs are highly expressed in the brain where they play roles in directing neurons during brain development, neuronal differentiation, and synaptogenesis [Akins



and Biederer, 2006]. Although clustered PCDHs are suspected to have more important roles than non-clustered PCDHs in neuronal development, human diseases that are associated with clustered PCDHs have not yet been reported. The genomic organization of *PCDHA* and *PCDHG* includes multiple variable exons and a set of constant exons, similar to the gene encoding immunoglobulins and T-cell receptors [Morishita and Yagi, 2007; Takeichi, 2007]. These exons are combined by cis-splicing of the mRNA, leading to the production of a large number of isoforms and generating more than 50 transcripts from each gene, with various extracellular domain sequences [Morishita and Yagi, 2007; Takeichi, 2007]. Because of these characteristics, *PCDHA* and *PCDHG* are classified as clustered PCDHs. The expression mechanism of clustered PCDHs is also unique; different mouse neurons were found to express different sets of *Pcdha* and *Pcdhg*, indicating monoallelic gene expression that is unique to the clustered PCDHs [Esumi et al., 2005; Hirayama and Yagi, 2006].

Although mutations of human *PCDHA*, *PCDHB*, and *PCDHG* have not been reported, hypomorphic *Pcdha* mutant mice exhibit enhanced contextual fear conditioning and abnormal spatial learning [Fukuda et al., 2008]. Morpholino-based reduction in levels of full-length *Pcdh1a* protein results in a dramatic increase in the extent of neuronal programmed cell death [Emond and Jontes, 2008]. These observations are similar to those in *Pcdhg*<sup>-/-</sup> mice that exhibit a loss of spinal interneurons [Wang et al., 2002]. Heterozygous mice of both *Pcdha* and *Pcdhg* have not been reported to show any neurological pathologies [Wang et al., 2002; Fukuda et al., 2008]; however, functional relevance of both *PCDHA* and *PCDHG* to human disorders cannot be denied, because mice heterozygous for the knockout alleles such as *Nsd1* and *Foxc1* show no manifestations [Rayasam et al., 2003; Aldinger et al., 2009]. Hemi-allelic deletions of the human homologues, *NSD1* and *FOXC1*, are associated with human disorders, i.e., Sotos syndrome and Dandy-Walker malformation, respectively. These findings suggest the biological difference between mice and human.

Another study showed that myelination functions as a trigger for the decline in *Pcdha* expression [Morishita et al., 2004]. Delayed myelination was another characteristic of our patients and may be associated with the deletions of *PCDHA*. Furthermore, *PCDHA* and *PCDHG* exhibit monoallelic expression [Esumi et al., 2005]. Thus, partial monosomy of 5q31.3 may affect the function of *PCDHA* and/or *PCDHG*.

By use of the UCSC genome browser, 6 genes other than *PCDHA* and *PCDHG* were found to be highly expressed in the brain among the 40 genes included in the common deletion region (Supplemental Table S1 online). Neuregulin 2 gene (*NRG2*) was one of the 6 genes. *NRG2* is a member of the neuregulin family of signaling proteins that mediate cell-cell interactions in the nervous system and other organs [Rimer, 2007]. Recent genetic, transgenic, and postmortem brain studies support a potential contribution of *NRG1*-erbB4 signaling in schizophrenia [Banerjee et al., 2010]. Furthermore, *NRG2* is predominantly expressed by neurons in the central nervous system and exerts its effects on the perisynaptic Schwann cells at the neuromuscular junction [Longart et al., 2004; Rimer, 2007], suggesting a possible association of *NRG2* with neurological diseases. The findings of histological examinations of

the brain of *Nrg2* transgenic mice did not differ from those of the wild-type or heterozygous mice; however, homozygous knockout mice showed severe growth retardation, increased morbidity, and reduced reproductive capacity [Britto et al., 2004]. Thus, the peripheral neuropathy in Patient 1 may be attributable to *NRG2* deletion.

In this study, we reported the first two patients with deletions of the 5q31.3 region. We suggest that the deletion of 5q31.3, including clustered PCDHs and *NRG2*, lead to severe developmental delays, distinctive facial features, and delayed myelination. These characteristic manifestations comprise a new recognizable microdeletion syndrome. Although many genes in this region are highly expressed in the brain, the genes that specifically contributed to the unique characteristics of our patients could not be determined, because the crucial functions of the genes involved in the deletion region remain to be elucidated. Further studies need to be conducted to identify the genes that were associated with the characteristic features of our patients. Microcephaly was observed in Patient 1, but the head circumference of Patient 2 was within normal limit. Therefore, the gene associated with microcephaly in Patient 1 might be excluded from the deletion region that was common to both patients.

## ACKNOWLEDGMENTS

Dr. Shimojima thanks Hayashi Memorial Foundation for Female Natural Scientists for the grant aid support. We also would like to acknowledge the DECIPHER database for bringing together similar patients from different groups.

## REFERENCES

- Akins MR, Biederer T. 2006. Cell–cell interactions in synaptogenesis. *Curr Opin Neurobiol* 16:83–89.
- Aldinger KA, Lehmann OJ, Hudgins L, Chizhikov VV, Bassuk AG, Ades LC, Krantz ID, Dobyns WB, Millen KJ. 2009. FOXC1 is required for normal cerebellar development and is a major contributor to chromosome 6p25.3 Dandy–Walker malformation. *Nat Genet* 41:1037–1042.
- Arens YH, Engelen JJ, Govaerts LC, van Ravenswaay CM, Loneus WH, van Lent-Albrechts JC, van der Blij-Philipsen M, Hamers AJ, Schrandt-Stumpel CT. 2004. Familial insertion (3;5)(q25.3;q22.1q31.3) with deletion or duplication of chromosome region 5q22.1–5q31.3 in ten unbalanced carriers. *Am J Med Genet Part A* 130A:128–133.
- Banerjee A, Macdonald ML, Borgmann-Winter KE, Hahn CG. 2010. Neuregulin 1-erbB4 pathway in schizophrenia: From genes to an interactome. *Brain Res Bull* 83:132–139.
- Britto JM, Lukehurst S, Weller R, Fraser C, Qiu Y, Hertzog P, Busfield SJ. 2004. Generation and characterization of neuregulin-2-deficient mice. *Mol Cell Biol* 24:8221–8226.
- Emond MR, Jontes JD. 2008. Inhibition of protocadherin- $\alpha$  function results in neuronal death in the developing zebrafish. *Dev Biol* 321:175–187.
- Esumi S, Kakazu N, Taguchi Y, Hirayama T, Sasaki A, Hirabayashi T, Koide T, Kitsukawa T, Hamada S, Yagi T. 2005. Monoallelic yet combinatorial expression of variable exons of the protocadherin- $\alpha$  gene cluster in single neurons. *Nat Genet* 37:171–176.
- Felding I, Kristoffersson U. 1980. A child with interstitial deletion of chromosome No. 5. *Hereditas* 93:337–339.
- Fukuda E, Hamada S, Hasegawa S, Katori S, Sanbo M, Miyakawa T, Yamamoto T, Yamamoto H, Hirabayashi T, Yagi T. 2008. Down-regulation of protocadherin- $\alpha$  isoforms in mice changes contextual fear conditioning and spatial working memory. *Eur J Neurosci* 28:1362–1376.
- Garcia-Minaur S, Ramsay J, Grace E, Minns RA, Myles LM, FitzPatrick DR. 2005. Interstitial deletion of the long arm of chromosome 5 in a boy with multiple congenital anomalies and mental retardation: Molecular characterization of the deleted region to 5q22.3q23.3. *Am J Med Genet Part A* 132A:402–410.
- Hirayama T, Yagi T. 2006. The role and expression of the protocadherin- $\alpha$  clusters in the CNS. *Curr Opin Neurobiol* 16:336–342.
- Komoike Y, Shimojima K, Liang JS, Fujii H, Maegaki Y, Osawa M, Fujii S, Higashinakagawa T, Yamamoto T. 2010. A functional analysis of GABARAP on 17p13.1 by knockdown zebrafish. *J Hum Genet* 55:155–162.
- Kramer RL, Feldman B, Ebrahim SA, Kasperski SB, Johnson MP, Evans ML. 1999. Molecular cytogenetic analysis of a de novo 5q31q33 deletion associated multiple congenital anomalies: Case report. *Am J Med Genet* 82:143–145.
- Longart M, Liu Y, Karavanova I, Buonanno A. 2004. Neuregulin-2 is developmentally regulated and targeted to dendrites of central neurons. *J Comp Neurol* 472:156–172.
- Morishita H, Kawaguchi M, Murata Y, Seiwa C, Hamada S, Asou H, Yagi T. 2004. Myelination triggers local loss of axonal CNR/protocadherin  $\alpha$  family protein expression. *Eur J Neurosci* 20:2843–2847.
- Morishita H, Yagi T. 2007. Protocadherin family: Diversity, structure, and function. *Curr Opin Cell Biol* 19:584–592.
- Mosca AL, Callier P, Leheup B, Marle N, Jalloul M, Coffinet L, Feillet F, Valduga M, Jonveaux P, Mugneret F. 2007. Fortuitous FISH diagnosis of an interstitial microdeletion (5)(q31.1q31.2) in a girl suspected to present a cri-du-chat syndrome. *Am J Med Genet Part A* 143A:1342–1347.
- Rayasam GV, Wendling O, Angrand PO, Mark M, Niederreither K, Song L, Lerouge T, Hager GL, Chambon P, Losson R. 2003. NSD1 is essential for early post-implantation development and has a catalytically active SET domain. *EMBO J* 22:3153–3163.
- Rimer M. 2007. Neuregulins at the neuromuscular synapse: Past, present, and future. *J Neurosci Res* 85:1827–1833.
- Takeichi M. 2007. The cadherin superfamily in neuronal connections and interactions. *Nat Rev Neurosci* 8:11–20.
- Tzschach A, Krause-Plonka I, Menzel C, Kalscheuer V, Toennies H, Scherthan H, Knoblauch A, Radke M, Ropers HH, Hoeltzenbein M. 2006. Molecular cytogenetic analysis of a de novo interstitial deletion of 5q23.3q31.2 and its phenotypic consequences. *Am J Med Genet Part A* 140A:496–502.
- Visser R, Matsumoto N. 2003. Genetics of Sotos syndrome. *Curr Opin Pediatr* 15:598–606.
- Wang X, Weiner JA, Levi S, Craig AM, Bradley A, Sanes JR. 2002. Gamma protocadherins are required for survival of spinal interneurons. *Neuron* 36:843–854.
- Yagi T. 2008. Clustered protocadherin family. *Dev Growth Differ* 50: S131–140.

## Original Article

# Immunohistochemical expression of fibroblast growth factor-2 in developing human cerebrum and epilepsy-associated malformations of cortical development

Manami Ueda,<sup>1</sup> Chitose Sugiura,<sup>2</sup> Kousaku Ohno,<sup>2</sup> Akiyoshi Kakita,<sup>3</sup> Akira Hori,<sup>4,7</sup> Eisaku Ohama,<sup>5</sup> Harry V. Vinters<sup>8,9</sup> and Hajime Miyata<sup>6</sup>

Divisions of <sup>1</sup>Neuropathology and <sup>2</sup>Child Neurology, Department of Neurological Sciences, Graduate School of Medical Sciences, Tottori University, Yonago, <sup>3</sup>Department of Pathological Neuroscience, Resource Branch for Brain Disease Research, CBBR, Brain Research Institute, Niigata University, Niigata, <sup>4</sup>Research Institute for Longevity Medicine, Fukushima Hospital, Toyohashi, <sup>5</sup>Kurashiki Heisei Hospital, Kurashiki, <sup>6</sup>Department of Neuropathology, Research Institute for Brain and Blood Vessels – Akita, Akita, Japan, <sup>7</sup>Department of Pathology, Medizinische Hochschule Hannover, Hannover, Germany, Departments of <sup>8</sup>Pathology and Laboratory Medicine (Neuropathology) and <sup>9</sup>Neurology, David Geffen School of Medicine and UCLA Medical Center, Los Angeles, California, USA

**To elucidate the biological significance of fibroblast growth factor-2 (FGF-2) expression in epilepsy-associated malformations of cortical development, immunohistochemical expression of FGF-2 was investigated in the developing human cerebral mantles obtained from 30 autopsy cases of fetuses, stillborn infants and children ranging from 12 weeks gestation to 15 years old, and 70 surgically-resected corticectomy specimens from patients with medically intractable epilepsy, including: group I, 12 tubers of tuberous sclerosis; group II, 24 cases of focal cortical dysplasia (FCD) with balloon cells (BC); group III, 11 FCD without BC; group IV, 23 histologically normal-appearing neocortices from patients with Rasmussen encephalitis, cystic-gliotic encephalopathy, temporal lobe epilepsy; and group V, 14 normal-appearing neocortices adjacent to dysplastic lesions from groups I and II. FGF-2 expression was detected in a population of matrix cells and/or neuroblasts within the ventricular zone in fetuses younger than 19 weeks gestation. Nuclei of glioblasts and immature astrocytes were also positive for FGF-2 in cases older than 18 weeks gestation. FGF-2 expression was not detected in immature cortical plate**

**neurons. Astrocytes and ependymal cells were positive for FGF-2 in the postnatal brains. Choroid plexus epithelium was strongly positive for FGF-2 in all cases examined. Among the corticectomy specimens, the cytoplasm and/or nuclei of dysmorphic neurons (DNs) and BCs in groups I and II were variably positive for FGF-2. The proportions of FGF-2 immunoreactive cells (FGF-2-IR%) was significantly higher in groups I (36.9 ± 9.6) and II (45.1 ± 7.0) than in groups III (21.0 ± 5.7), IV (14.4 ± 4.7) and V (24.3 ± 10.3), and that in group V was higher than in group IV ( $P < 0.01$ ). These results indicate that FGF-2 upregulation in DN and BCs is an important feature common to groups I and II, and suggest that BCs and DN in these groups represent disturbed gliogenesis from matrix cells and disturbed maturation of cortical neurons from migrating neuroblasts, respectively.**

**Key words:** astrocyte, epilepsy, FGF-2, immunohistochemistry, malformation of cortical development (MCD).

## INTRODUCTION

Malformations of cortical development (MCDs) constitute a family of disorders characterized by an abnormal cytoarchitecture of the cerebral cortex, presumably resulting from deranged migration of neuroblasts from ventricular and subventricular zones (VZ and SVZ, respectively) to

Correspondence: Hajime Miyata, MD, PhD, Department of Neuropathology, Research Institute for Brain and Blood Vessels – Akita, 6-10 Senshu-Kubota-Machi, Akita 010-0874, Japan. Email: hmiyata-nsu@umin.ac.jp

Received 1 December 2010; revised and accepted 3 January 2011; published online 7 March 2011.

the cortical plate during early stages of intrauterine life.<sup>1</sup> Focal cortical dysplasia (FCD),<sup>2</sup> a subset of MCDs, is characterized by cortical laminar disorganization, the presence of dysmorphic neurons (DNs) and characteristic large gemistocytic astrocyte-like “balloon cells” (BCs), histologically classified as FCD type IIB<sup>3</sup> or FCD type Iib<sup>4</sup> in recent proposals. These histological features are very similar to those seen in cortical tubers of tuberous sclerosis complex (TSC-tubers),<sup>5,6</sup> despite different clinical presentations. TSC-tubers and FCD type Iib are presumed to be disorders of cell differentiation in early stages of the developing brain.<sup>7</sup> Recent evidence has suggested several factors significant in morphogenesis of BCs, including aberrant expression of cytoskeletal proteins,<sup>8,9</sup> stem cell markers such as nestin,<sup>10</sup> and CD34 class II,<sup>11</sup> and altered signaling pathways.<sup>12,13</sup> However, the origin of BCs is largely unknown.

The fibroblast growth factor (FGF) family consists of at least 23 different members, having two highly conserved core-domain regions.<sup>14,15</sup> Ten of 23 classes of the FGF family along with four receptors are expressed in the developing brain in animals.<sup>14</sup> Among them FGF-2 has been suggested to play several important roles not only in neuroprotection following brain insults such as ischemia,<sup>16–18</sup> traumatic injury,<sup>19,20</sup> and epilepsy,<sup>21,22</sup> but also in neurogenesis<sup>23–25</sup> and neuronal and glial differentiation<sup>26,27</sup> in the developing CNS. Our previous study using a relatively small number of cases has demonstrated that FGF-2 is expressed in the nuclei of astrocytes in normal-appearing neocortex, and DN and BCs in TSC-tubers and FCD with BC but not in FCD without BC, and that higher proportions of FGF-2 immunoreactive cells (FGF-2-IR%) in TSC-tubers and FCD with BC than FCD without BC may reflect the likely timing of insults underlying the pathogenesis of each disorder.<sup>28</sup> However, the spatial and temporal alterations of FGF-2 expression in the developing human brain have not yet been fully described in the literature. One study has demonstrated FGF-2 expression in both neuroblasts and glioblasts in the cortical plate using human fetal brains of 12 to 16 weeks gestation.<sup>29</sup> In rat brain, FGF-2 expression has been shown in VZ, SVZ and cerebral cortex at the embryonic day (E18),<sup>30</sup> and subsequently in astrocytes but not neurons, except those in the hippocampus and cingulate cortex in the postnatal period.<sup>31,32</sup>

In the present study, immunohistochemical expression of FGF-2 was investigated in 30 autopsy cases of the developing human cerebrum and 70 surgically resected corticectomy specimens from patients with medically intractable epilepsy using tissue microarray for the quantitative evaluation of FGF-2-IR% to elucidate the biological significance of FGF-2 expression in epilepsy-associated MCDs.

## MATERIALS AND METHODS

### Population characteristics

#### *Autopsied human developing brains*

Archival paraffin blocks from 30 autopsy brains of human fetuses, stillborn infants and children ranging from 12 weeks gestation to 15 years old were retrospectively chosen for this study. Histologically normal areas of the cerebral mantle were selected for immunohistochemical assessment (Table 1). The term “histologically normal” refers to histologically normal-appearing tissue, regardless of its functional state, in which there are no histological changes observed by HE staining in a given case.

#### *Epilepsy-associated brain lesions*

Seventy surgically-resected specimens from patients (M : F = 35:35; age at time of surgery ranging from 10 weeks to 49 years; mean, 14.9 ± 14.3 years) with medically intractable epilepsy or infantile spasms were retrospectively chosen for this study from archival paraffin blocks. These include tissue in the following group categories: (I) cortical tuber of tuberous sclerosis complex (TSC-tuber) ( $n = 12$ ; M : F = 5:7; age range, 1–27 years; mean, 10.3 ± 9.7 years); (II) focal cortical dysplasia (FCD) with balloon cell (BC) ( $n = 24$ ; M : F = 12:12; age range, 11 weeks to 45 years; mean, 12.2 ± 14.5 years); (III) FCD without BC ( $n = 11$ ; M : F = 6:5; age range, 10 weeks to 25 years; mean, 6.9 ± 9.6 years); (IV) 23 cases of histologically normal neocortex (N-CTX) obtained from pathologically confirmed (IV-1) Rasmussen encephalitis ( $n = 5$ ; M : F = 2:3; age range, 3–9 years; mean, 6.0 ± 2.5 years), (IV-2) cystic-gliotic encephalopathy ( $n = 2$ , M : F = 0:2; age range, 8–10 years; mean, 9 ± 1.4 years), (IV-3) mesial temporal lobe epilepsy with or without hippocampal sclerosis ( $n = 16$ ; M : F = 10:6; age range, 9–49 years; mean, 31.3 ± 12.1 years); and (V) 14 cases of normal-appearing neocortex adjacent to dysplastic lesions (Ad-CTX) obtained from eight and six specimens in categories I and II, respectively ( $n = 14$ ; M : F = 8:6; age range, 9 months to 42 years; mean, 14.8 ± 12.4 years). All patients in group I fulfilled the diagnostic criteria for clinically definite TSC.<sup>33</sup> The pathological diagnosis of FCD with BC was made on specimens from patients who had no signs or systemic manifestations of TSC (so-called isolated CD), and represent “severe” FCD in the previously described classification and proposed grading system,<sup>34</sup> equivalent to FCD type IIB<sup>3</sup> and FCD type Iib.<sup>4</sup> The diagnosis of CD without BC also represents isolated CD, but no BCs were observed even by extensive sampling of resected tissue, that include FCD type IB ( $n = 3$ ) and IIA ( $n = 8$ ) in this study.<sup>3</sup> The term “histologically normal” cortex refers to histologically normal-appearing cortex, regardless of its



**Table 1** Clinicopathological summary of the 30 autopsy cases

Case no.	Age	Sex	Clinical diagnosis	Pathological diagnosis
1	12 w	U	Thoracoomphalopagus	Complete agenesis of the corpus callosum
2	12 w	U	Thoracoomphalopagus	Complete agenesis of the corpus callosum
3	13 w	F	Not described	Normal brain for age
4	16 w	F	Trisomy 18 syndrome	Trisomy 18 syndrome
5	18 w	M	Meckel-Gruber syndrome	Meckel-Gruber syndrome
6	19 w	M	Trisomy 18 syndrome	Trisomy 18 syndrome
7	20 w	F	Abortion due to uterus bicornis	Normal brain for age
8	20 w	F	Abortion due to uterus bicornis	Normal brain for age
9	20 w	F	Hunter syndrome	Hunter syndrome
10	21 w	U	Defect of lower limbs	Focal cortical dysplasia
11	21 w	F	Cardiac abnormality	Normal brain for age
12	24 w	F	Cystic hygroma colli	Dysplasia of the cerebral and cerebellar cortices
13	24 w	M	Hypophosphatasia	Normal brain for age
14	30 w	M	Fetal hydrops	Fresh multiple periventricular hemorrhages
15	33 w	F	69XXX	Dysgenesis of the central nervous system
16	34 w	M	Trisomy 18 syndrome	Trisomy 18 syndrome
17	38 w	U	Asphyxia due to rotation abnormality	Congestive brain
18	38 w	F	Congenital cardiac disease	Congestive brain, dysplasia of the hippocampus
19	7 m	F	Sudden infant death syndrome	Congenital cytomegalovirus infection
20	10 m	F	Hemophagocytic syndrome	Infiltration of histiocytes in the subarachnoid space
21	12 m	M	Sudden infant death syndrome	Dysplasia of the brain
22	15 m	F	Hydrencephalus after brain hemorrhage	Hydrencephalus, old subependymal hemorrhage
23	4 y	F	Developmental disorder	Developmental disorder
24	5 y	F	Developmental disorder, sudden death	Dysplasia of the brain
25	6 y	F	Ependymoma in the fourth ventricle	Anaplastic ependymoma, Grade III
26	6 y	M	Menkes kinky hair disease	Menkes kinky hair disease
27	9 y	F	Holoprosencephaly	Holoprosencephaly
28	10 y	F	Medulloblastoma	Medulloblastoma
29	12 y	F	Death by drowning	Dysplastic brain
30	15 y	M	Status epilepticus	Hepatic encephalopathy

F, female; M, male; m, month(s) old; U, unknown; w, weeks gestation; y, year(s) old.

functional state, in which there are no histological changes observed by HE staining that presented adjacent to the specific lesion. No two specimens came from the same individual except those in Group V. Tissues of 62 cases are already included in a tissue microarray paraffin block originally containing 63 cases used in the previous study,<sup>13</sup> with one case of cystic-gliotic encephalopathy excluded due to insufficient amount of tissue remaining within the block. Paraffin blocks of eight cases (4 TSC-tubers, 2 FCD with BC, 2 FCD without BC) not allowed to be incorporated into the tissue microarray were also included in this study by defining a region of interest in each case throughout the study.

### Histological and immunohistochemical procedures

Paraffin blocks were cut at 5  $\mu$ m thickness, subjected to HE and KB staining as routine procedures. Adjacent serial sections were subjected to immunohistochemistry for FGF-2 and GFAP. For FGF-2 immunostaining, deparaffinized sections were subjected to autoclave boiling in 0.015 mol sodium citrate buffer solution (pH 6.0) for 10 min at 121°C as an antigen retrieval procedure before incubation with 3% H<sub>2</sub>O<sub>2</sub> diluted in distilled water for

30 min followed by blocking with 5% normal goat serum. Sections were incubated with rabbit polyclonal antibodies for FGF-2 (dilution 1:50, Santa Cruz Biotechnology, Santa Cruz, CA, USA) or rabbit polyclonal antibodies for GFAP (dilution 1:300, Dako, Glostrup, Denmark) overnight at 4°C, followed by incubation with goat anti-rabbit immunoglobulins conjugated to peroxidase labeled-dextran polymer (EnVision+ System-HRP, Dako, Carpinteria, CA, USA) for 45 min at 37°C. Immunoreaction was visualized by 3–3'-diaminobenzidine tetrahydrochloride (DAB, Dako, Carpinteria, CA, USA). Sections were counterstained with hematoxylin. Immunostaining with omission of primary antibodies was used as a negative control. Fibroblasts in human leptomeninges were used as built-in positive control for FGF-2.

### Semi-quantitative analysis of FGF-2 immunoreactivity in MCDs

The histology of all cores in tissue microarray was verified on HE-stained sections to confirm that a region of interest from a donor block appeared in a given core (round tissue with 600  $\mu$ m diameter, approximately 0.28 mm<sup>2</sup>). Cores lost or severely damaged during staining were excluded from the study. Immunoreactivity was judged as positive regard-

less of staining intensity, when DAB signal in a given cell was higher than the background. Any cells within blood vessels or their walls, for example, vascular endothelial and smooth muscle cells, were excluded from the study. Only cells with the nucleus in the plane of the section were counted. The computer-assisted semi-quantitative analysis of FGF-2 immunoreactivity on tissue microarray was performed according to the previously described protocol.<sup>13</sup> For another eight cases that are not included in the tissue microarray, seven consecutive areas of interest (AOIs) were determined using a 40X objective lens (approximately 1.58 mm<sup>2</sup>) based on the HE stained sections in each case for the semi-quantitative evaluation of FGF-2 expression.<sup>28</sup> The proportion of FGF-2 immunoreactive cells (FGF-IR%) in a given specimen was measured by counting all FGF-2 immunoreactive neuroglial cells divided by total number of cells in each core and AOI. The mean values of the positive ratio from each group were statistically compared by analysis of variance (ANOVA) followed by a post hoc Scheffe's test for multiple comparisons. The statistical difference was considered to be significant when  $P < 0.01$ .

## RESULTS

### FGF-2 expression in developing human brain

Weak or faint FGF-2 immunoreaction was observed and almost confined to a population of what appeared to be matrix cells and/or neuroblasts within the VZ in all five fetuses from 12 to 18 weeks gestation (Fig. 1A). In fetuses of 19 weeks gestation or older, nuclei of what seemed to be glioblasts and immature astrocytes within SVZ and intermediate zone (IMZ) as well as immature cells within the VZ and ependymal layer were variably immunoreactive for FGF-2 (Fig. 1B,C). Fetal immature ependymal cells were strongly immunoreactive for FGF-2 in their cytoplasm (Fig. 1C), while mature ependymal cells with ciliated cuboidal morphology, particularly in the postnatal brains, showed FGF-2 expression more localized in the apical brush border (Fig. 1D). The spatial and temporal alterations of FGF-2 expression in these developing human brains were almost parallel with those of GFAP expression, except the cortical plate and choroid plexus; that is, no FGF-2 immunoreactivity was observed in astrocytes and immature neurons in the cortical plate in all fetal cases (Fig. 1E), despite few GFAP-positive astrocytes scattered in the cortical plate in fetal brains of 19 weeks gestation or older. However, in 8/12 postnatal brains from infants and children, faint immunoreactivity of FGF-2 was observed in a population of cortical astrocytes, and nuclei and/or cytoplasm of GFAP-positive astrocytes in the subependymal layer and white matter were variably immunoreactive

for FGF-2 (Fig. 1F). FGF-2 immunoreactivity was not detected in the neocortical neurons in any of the autopsy cases examined in the present study. Cytoplasm of choroid plexus epithelium was strongly positive for FGF-2 in all cases examined (Fig. 1D) (Table 2).

### FGF-2 immunoreactivity in MCDs and the proportions of FGF-2 immunoreactive cells

In cases from groups I (TSC-tubers) and II (FCD with BC), abnormal neuroglial cells including DN and BCs were variably immunoreactive for FGF-2 (Fig. 2A,B). In contrast, no or very subtle, if any, FGF-2 immunoreactivity was detected in the neuronal component including, DN in cases from group III (FCD without BC) (Fig. 2C). The cytoplasm and/or nuclei of both normal-appearing and reactive astrocytes was positive for FGF-2 in all cases (Fig. 2C,D) from all groups including group V (Ad-CTX). All of these findings were consistent with our previous study.<sup>28</sup> FGF-2 immunoreactivity was not detected in normal and normal-appearing neurons in cases from groups IV and V. The proportions of FGF-2-IR% were significantly higher in groups I (mean  $\pm$  SD: 36.9  $\pm$  9.6) and II (45.1  $\pm$  7.0) than in groups III (21.0  $\pm$  5.7), IV (14.4  $\pm$  4.7) and V (24.3  $\pm$  10.3) with statistical significance ( $P \leq 0.0017$ ) (Fig. 3), and that in group V was higher than in group IV with statistical significance ( $P = 0.0062$ ) (Fig. 3). There was no significant difference in the FGF-2-IR% between groups I and II ( $P = 0.0534$ ), III and IV ( $P = 0.2181$ ) and III and V ( $P = 0.8726$ ).

## DISCUSSION

### FGF-2 expression is associated with gliogenesis from matrix cells to astrocytes

The observations in the present study indicate the transition of FGF-2 expression from matrix cells to glioblasts and astrocytes during human brain development. FGF-2 immunoreactive cells in VZ and SVZ before 19 weeks gestation may represent matrix cells and/or neuroblasts when glioblasts are not yet generated, although there are no specific immunohistochemical markers applicable to formalin-fixed paraffin-embedded human autopsy brain tissue to identify matrix cells, neuroblasts and glioblasts. However, FGF-2 immunoreactivity was not observed in neuroblasts and/or immature neurons in the cortical plate migrated from VZ/SVZ in the present study, although FGF-2 expression has also been demonstrated in both neuroblasts and glioblasts in the cortical plate using frozen sections from human fetal brains of 12–16 weeks gestation.<sup>29</sup> On the other hand, FGF-2 expression was observed in nuclei of GFAP-expressing astrocytes in IMZ or white

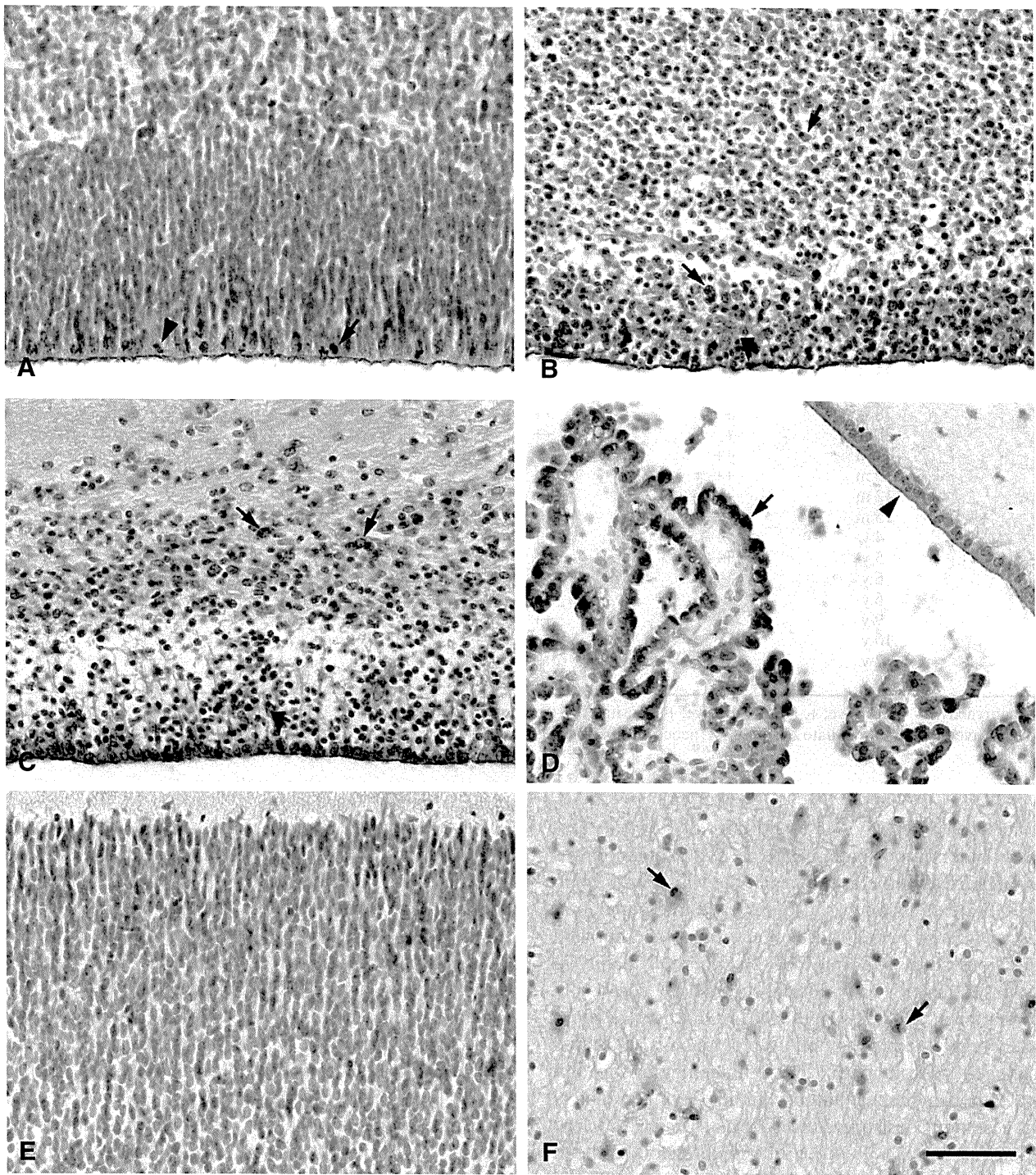


**Fig. 1** Fibroblast growth factor (FGF)-2 expression in developing human cerebrum. (A) Weak or faint FGF-2 immunoreactivity almost confined to a population of what appeared to be matrix cells and/or neuroblasts within the ventricular zone (VZ: arrow) in a fetal brain of 12 weeks gestation. Note scattered mitotic figures within the VZ (arrowhead). (B) Nuclei of what seem to be glioblasts and immature astrocytes (arrows) within the subventricular zone (SVZ) as well as immature cells within the VZ and ependymal layer (arrowhead) are variably immunoreactive for FGF-2. A fetal brain of 21 weeks gestation. (C) In addition to the positive reaction for FGF-2 in glioblasts (arrows), immature ependymal cells are strongly immunoreactive for FGF-2 in their cytoplasm (arrowhead). A 21 weeks gestation fetus. (D) Cytoplasm of the choroid plexus epithelium is strongly positive for FGF-2 in all cases examined (arrow). Mature ependymal cells with ciliated cuboidal morphology, particularly in the postnatal brains showed FGF-2 expression more localized in the apical brush border (arrowhead). A 7-month-old infant. (E) No FGF-2 immunoreactivity was observed in the cortical plate in all fetal cases. A 12 weeks gestation fetus. (F) Nuclei and/or cytoplasm of reactive astrocytes in the white matter are positive for FGF-2 (arrows). A 7-month-old infant. All panels were photographed at the same magnification. Bar = 50  $\mu$ m.

**Table 2** Summary of FGF-2 immunoreactivity in developing human cerebra

Case No.	Age	VZ/EL	SVZ/SEL	IMZ/WM	CP/NCTX	CPE
1	12 w	+	-	-	-	+++
2	12 w	+	-	-	-	+++
3	13 w	+	-	-	-	+++
4	16 w	++	-	-	-	+++
5	18 w	+	-	-	-	+++
6	19 w	++	+	+	-	+++
7	20 w	++	-	-	-	+++
8	20 w	++	++	+	-	+++
9	20 w	++	++	-	-	+++
10	21 w	++	++	+	-	+++
11	21 w	+++	++	+	-	+++
12	24 w	+	-	-	-	++
13	24 w	+	+	+	-	++
14	30 w	+	+	+	-	+++
15	33 w	+	+	+	-	+++
16	34 w	+	+	+	-	+++
17	38 w	+	++	++	-	+++
18	38 w	+	++	++	-	+++
19	7 m	++	++	++	+	+++
20	10 m	++	++	++	+	+++
21	12 m	++	++	++	+	+++
22	15 m	++	++	++	-	+++
23	4 y	+++	++	++	+	+++
24	5 y	+++	++	++	-	+++
25	6 y	++	++	++	-	+++
26	6 y	++	++	++	+	+++
27	9 y	++	++	++	+	+++
28	10 y	++	++	++	+	+++
29	12 y	+	++	++	-	+++
30	15 y	++	++	++	+	++

Immunoreactivity: -, negative; +, faintly positive; ++, positive; +++, strongly positive. CP, cortical plate; CPE, choroid plexus epithelium; EL, ependymal layer; IMZ, intermediate zone; NCTX, neocortex; SEL, subependymal layer; SVZ, subventricular zone; VZ, ventricular zone; WM, white matter.

matter as well as VZ/SVZ in fetal brains of 19 weeks gestation or older. In postnatal brains, FGF-2 expression was mainly observed in the astrocytes in the white matter and faint FGF-2 expression was also observed in a population of neocortical astrocytes. These observations, together with the previous study showing FGF-2 expression mainly in astrocytes in histologically normal cerebral neocortex and white matter in adults,<sup>28</sup> suggest that FGF-2 is a developmentally regulated protein and its expression is associated with gliogenesis from matrix cells in human brain development. Although human autopsy brains younger than 9 weeks gestation consisting entirely of matrix cells were not available in this study, FGF-2 mRNA expression has been observed in cells in neural tubes at embryonic day E10 in mice, when neural crest precursors proliferate.<sup>35</sup> In fact, FGF-2 has been detected in astrocytes but not neurons, except those in CA2 of the hippocampus in normal postnatal and adult rat brains.<sup>31,32</sup> Hence, FGF-2 expression in abnormal neuroglial cells, particularly DNs in cases of MCD with BC (groups I and II), in the present study appears to represent one immature feature of these cells,<sup>1</sup> and reflects the putative perturbations of developmental events in the early fetal period underlying the pathogenesis

of these dysplastic lesions.<sup>28</sup> Accordingly MCD with BC may differ from FCD without BC (group III) in the likely timing of insults underlying the pathogenesis of each disorder, despite the presence of morphologically identical DNs in these lesions. Although the presence of BCs is one histological hallmark of groups I and II, BCs may not always intermingle with DNs but also can exist as isolated small aggregates within the adjacent normal-appearing cortex and white matter.<sup>4-6,13</sup> In such situation, the presence of FGF-2 immunoreactive DNs may therefore even indicate the presence of potentially "hidden" BCs in a given specimen, and could be one supplemental immunohistochemical feature for accurate and differential diagnosis of FCD type IIb from FCD type IIa.

### Possible role of FGF-2 in the pathogenesis of BCs

The present study has updated our preliminary report<sup>28</sup> on FGF-2-IR% in epilepsy-associated MCDs, demonstrating that FGF-2-IR% in BC-containing cortical dysplasia, that is, TSC-tubers and FCD with BC, is significantly higher than that in FCD without BC, and that FGF-2 upregulation



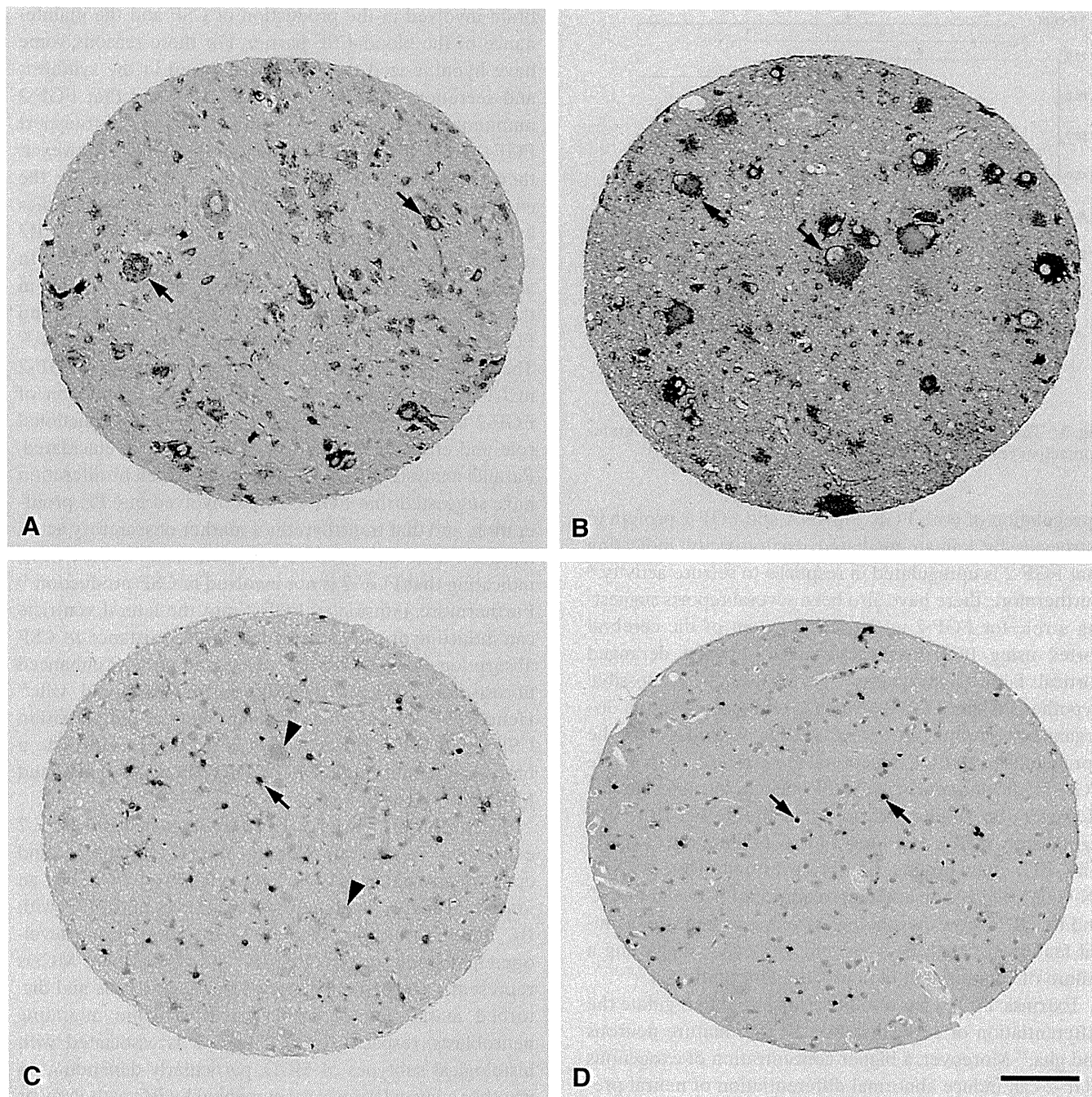


**Fig. 2** Tissue microarray immunohistochemistry for fibroblast growth factor (FGF)-2. Abnormal neuroglial cells are immunoreactive for FGF-2 in tuberous sclerosis complex (TSC)-tuber (panel A, arrows) and focal cortical dysplasia (FCD) with balloon cells (BC) (panel B, arrows). FGF-2 expression is observed in reactive astrocytes (arrow in panel C) but not in neuronal component including dysmorphic neurons in FCD without BC (arrowheads in panel C). In normal cerebral neocortex, nuclei and/or cytoplasm of astrocytes are positive for FGF-2 (panel D, arrows). All panels were photographed at the same magnification. Bar = 100  $\mu$ m.

appears to be an important feature common to TSC-tubers and FCD with BC. In addition, FGF-2-IR% in group V (Ad-CTX) was significantly higher than that in group IV (N-CTX), indicating that Ad-CTX is also abnormal in terms of FGF-2 expression. This difference appears to be mainly due to the difference in the proportion of FGF-2

immunoreactive normal and reactive astrocytes, since there were no DN or neuronal expression of FGF-2 observed in these groups.

Previous studies have demonstrated the upregulation of FGF-2 mRNA following bicuculline- or kainic acid-induced seizure mainly in the hippocampus,<sup>21,22</sup> and the

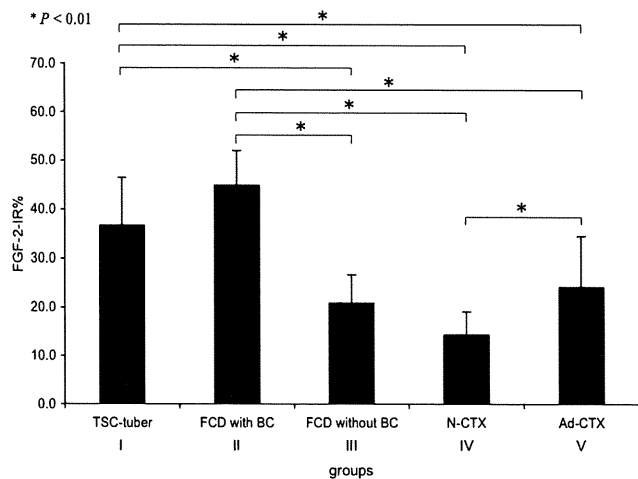


**Fig. 3** The ratios of fibroblast growth factor-2 (FGF-2) immunoreactive cells (FGF-2-IR%). \* $P < 0.01$ .

upregulation of both FGF-2 mRNA and FGF-2 protein in astrocytes by kainate-mediated excitotoxicity, indicating that FGF-2 is upregulated in response to seizure activity.<sup>36</sup> Furthermore, there have also been several reports suggesting a role for FGF-2 in the development of the cerebral cortex using FGF-2 knockout mice showing deranged cortical laminar structures.<sup>23–25</sup> Accordingly, a possible hypothesis is that FGF-2 protein is upregulated in the disorganized cerebral cortex of MCDs secondary to the upregulation of FGF receptors in response to possible FGF-2 deficiency during an early stage of intrauterine life. However, our results indicated that the FGF-2-IR% was significantly higher in groups I (TSC-tubers) and II (FCD with BC) than groups III (FCD without BC) and IV (N-CTX), suggesting a strong relationship between FGF-2 and BC. BCs show morphological and immunohistochemical features of both neurons and astrocytes, suggesting a failure of commitment in neuroglial differentiation.<sup>5,10,37</sup>

Extrinsic FGF-2 has also been suggested to regulate the differentiation of cortical stem cells into mature neurons and glia.<sup>27</sup> Moreover, a higher concentration of exogenous FGF-2 can induce abnormal differentiation of neural precursor cells into balloon-like cells expressing both GFAP and neurofilament.<sup>35</sup> Hence studies on the expressions of FGFR and FGF-2 mRNA in BCs would be helpful to further elucidate the histogenesis of BCs.

### Biological significance of FGF-2 immunoreactivity in choroid plexus epithelium

We demonstrated constant and strong immunoreactivity of FGF-2 in the choroid plexus epithelium (CPE) and moderate immunoreactivity in ependymal cells in all cases examined in the present study. The choroid plexuses (CPs) are specialized secretory tissues within the ventricle of the

brain involved in the production of CSF and the maintenance of the blood–CSF barrier. For these reasons, some have hypothesized that CPE is involved in the synthesis and secretion of FGF-2 into the CSF,<sup>38</sup> and that FGF-2 immunoreactive ependymal cells function to transport FGF-2 from the VZ into brain parenchyma.<sup>39</sup> However, there have been no reports to date demonstrating the expression of FGF-2 mRNA in CPs. Some previous studies have shown expression of FGFR1 mRNA and FGFR2 mRNA but no expression of FGF-2 mRNA in CPE.<sup>40,41</sup> In addition, expression of FGFR mRNA has been shown in the CPE of developing murine and adult rat brains,<sup>42,43</sup> and FGFR2 mRNA is highly expressed in the CPs in rats.<sup>44</sup> These results imply that strong immunoreactivity of FGF-2 in CPE represents the reception but not production of FGF-2 through FGFR on CPE. However, the functional role and effect of FGF-2 on CPE is yet to be elucidated. Parallel analysis of FGF-2 expression and cell proliferation have suggested that FGF-2 is not involved in CPE proliferation, and that transthyretin, a marker of secretory activity, is not affected by FGF-2 treatment using murine CPE, indicating that FGF-2 is not involved in CSF production.<sup>45</sup> Furthermore, infusion of FGF-2 into the lateral ventricle can induce hydrocephalus by increased resistance to CSF absorption, conceivably due, at least in part, to enhanced fibrosis and collagen deposits in the arachnoid villi.<sup>46</sup> Hence CPE may absorb excess amounts of FGF-2 within CSF via FGFRs. Further study is needed to elucidate a biological significance for FGF-2 in CNS development and MCDs as well as in CSF.

In conclusion, the present study demonstrates FGF-2 expression in the developing human cerebrum and epilepsy-associated MCDs. Upregulation of FGF-2 is an important feature common to TSC-tubers and FCD with BC, and the transition of FGF-2 expression in our developmental study suggests that BC and DN in these MCDs represent disturbed gliogenesis from matrix cells and disturbed maturation of cortical neurons from migrating neuroblasts, respectively. FGF-2-IR% is associated with histological subtypes of MCD, particularly depending on whether a given lesion is accompanied by BC pathology or not, reflecting the likely timing of insults underlying the pathogenesis of each disorder.

### ACKNOWLEDGEMENTS

Work presented in part at the Annual Meetings of the Japanese Society of Neuropathology (49th meeting at Tokyo, 2008 and 50th meeting at Takamatsu, 2009), and supported by Encouragement Fund for Graduate Students of Tottori University (MU), Grants-in-Aid for Scientific Research from the Ministry of Education, Culture, Sports, Science and Technology of Japan (17689040 (HM));

© 2011 Japanese Society of Neuropathology



18790717 (CS)), grants from the Japan Epilepsy Research Foundation (H16-009 and H21-004 (HM)) and a grant from the Collaborative Research Project (2011–2226 (HM, AK)) of the Brain Research Institute, Niigata University. HVV is supported in part by the Daljit S. & Elaine Sarkaria Chair in Diagnostic Medicine. Dr Gary W. Mathern (UCLA Medical Center) is a long-term collaborator. We thank Tomomi Araoka, Atsuko Iwata (Tottori University), Shuji Kato and Taeko Kaneko (Department of Neuropathology, Research Institute for Brain and Blood Vessels – Akita) for invaluable technical assistance.

## REFERENCES

- Cepeda C, André VM, Levine MS *et al.* Epileptogenesis in pediatric cortical dysplasia: the dysmature cerebral developmental hypothesis. *Epilepsy Behav* 2006; **9**: 219–235.
- Taylor DC, Falconer MA, Bruton CJ, Corsellis JA. Focal dysplasia of the cerebral cortex in epilepsy. *J Neurol Neurosurg Psychiatry* 1971; **34**: 369–387.
- Palmini A, Najm I, Avanzini G *et al.* Terminology and classification of the cortical dysplasias. *Neurology* 2004; **62** (Suppl 3): S2–S8.
- Blümcke I, Thom M, Aronica E *et al.* The clinicopathologic spectrum of focal cortical dysplasias: a consensus classification proposed by an ad hoc Task Force of the ILAE Diagnostic Methods Commission. *Epilepsia* 2011; **52**: 158–174.
- Crino PB, Miyata H, Vinters HV. Neurodevelopmental disorders as a cause of seizures: neuropathologic, genetic, and mechanistic considerations. *Brain Pathol* 2002; **12**: 212–233.
- Vinters HV, Miyata H. Neuropathologic features of tuberous sclerosis. In: McLendon RE, Rosenblum MK, Bigner DD, eds. *Russell & Rubinstein's Pathology of Tumors of the Nervous System*, 7th edn. London: Edward Arnold, 2006; 955–969.
- Barkovich AJ, Kuzniecky RI, Jackson GD, Guerrini R, Dobyns WB. A developmental and genetic classification for malformations of cortical development. *Neurology* 2005; **65**: 1873–1887.
- Mizoguchi M, Iwaki T, Morioka T, Fukui M, Tateishi J. Abnormal cytoarchitecture of cortical dysplasia verified by immunohistochemistry. *Clin Neuropathol* 1998; **17**: 100–109.
- Yamanouchi H, Jay V, Otsubo H, Kaga M, Becker LE, Takashima S. Early forms of microtubule-associated protein are strongly expressed in cortical dysplasia. *Acta Neuropathol* 1998; **95**: 466–470.
- Crino PB, Trojanowski JQ, Eberwine J. Internexin, MAP1B, and nestin in cortical dysplasia as markers of developmental maturity. *Acta Neuropathol* 1997; **93**: 619–627.
- Fausser S, Becker A, Schulze-Bonhage A *et al.* CD34-immunoreactive balloon cells in cortical malformations. *Acta Neuropathol* 2004; **108**: 272–278.
- Baybis M, Yu J, Lee A *et al.* mTOR cascade activation distinguishes tubers from focal cortical dysplasia. *Ann Neurol* 2004; **56**: 478–487.
- Miyata H, Chiang AC, Vinters HV. Insulin signaling pathways in cortical dysplasia and TSC-tubers: tissue microarray analysis. *Ann Neurol* 2004; **56**: 510–519.
- Reuss B, von Bohlen und Halbach O. Fibroblast growth factors and their receptors in the central nervous system. *Cell Tissue Res* 2003; **313**: 139–157.
- Ornitz DM. FGFs, heparan sulfate and FGFRs: complex interactions essential for development. *Bioessays* 2000; **22**: 108–112.
- Liu X, Zhu XZ. Increased expression and nuclear accumulation of basic fibroblast growth factor in primary cultured astrocytes following ischemic-like insults. *Brain Res Mol Brain Res* 1999; **71**: 171–177.
- Issa R, AlQteishat A, Mitsios N *et al.* Expression of basic fibroblast growth factor mRNA and protein in the human brain following ischaemic stroke. *Angiogenesis* 2005; **8**: 53–62.
- Leker RR, Soldner F, Velasco I, Gavin DK, Androutsellis-Theotokis A, McKay RD. Long-lasting regeneration after ischemia in the cerebral cortex. *Stroke* 2007; **38**: 153–161.
- Smith C, Berry M, Clarke WE, Logan A. Differential expression of fibroblast growth factor-2 and fibroblast growth factor receptor 1 in a scarring and nonscarring model of CNS injury in the rat. *Eur J Neurosci* 2001; **13**: 443–456.
- Leadbeater WE, Gonzalez AM, Logaras N, Berry M, Turnbull JE, Logan A. Intracellular trafficking in neurons and glia of fibroblast growth factor-2, fibroblast growth factor receptor 1 and heparan sulphate proteoglycans in the injured adult rat cerebral cortex. *J Neurochem* 2006; **96**: 1189–1200.
- Riva MA, Gale K, Mocchetti I. Basic fibroblast growth factor mRNA increases in specific brain regions following convulsive seizures. *Brain Res Mol Brain Res* 1992; **15**: 311–318.
- Riva MA, Donati E, Tascetta F, Zolli M, Racagni G. Short- and long-term induction of basic fibroblast growth factor gene expression in rat central nervous system following kainate injection. *Neuroscience* 1994; **59**: 55–65.
- Raballo R, Rhee J, Lyn-Cook R, Leckman JF, Schwartz ML, Vaccarino FM. Basic fibroblast growth factor (Fgf2) is necessary for cell proliferation and

- neurogenesis in the developing cerebral cortex. *J Neurosci* 2000; **20**: 5012–5023.
24. Ortega S, Ittmann M, Tsang SH, Ehrlich M, Basilico C. Neuronal defects and delayed wound healing in mice lacking fibroblast growth factor 2. *Proc Natl Acad Sci USA* 1998; **95**: 5672–5677.
  25. Dono R, Texido G, Dussel R, Ehmke H, Zeller R. Impaired cerebral cortex development and blood pressure regulation in FGF-2-deficient mice. *EMBO J* 1998; **17**: 4213–4225.
  26. Kilpatrick TJ, Bartlett PF. Cloning and growth of multipotential neural precursors: requirements for proliferation and differentiation. *Neuron* 1993; **10**: 255–265.
  27. Qian X, Davis AA, Goderie SK, Temple S. FGF2 concentration regulates the generation of neurons and glia from multipotent cortical stem cells. *Neuron* 1997; **18**: 81–93.
  28. Sugiura C, Miyata H, Ueda M, Ohama E, Vinters HV, Ohno K. Immunohistochemical expression of fibroblast growth factor (FGF)-2 in epilepsy-associated malformations of cortical development (MCDs). *Neuropathology* 2008; **28**: 372–381.
  29. Gonzalez AM, Hill DJ, Logan A, Maher PA, Baird A. Distribution of fibroblast growth factor (FGF)-2 and FGF receptor-1 messenger RNA expression and protein presence in the mid-trimester human fetus. *Pediatr Res* 1996; **39**: 375–385.
  30. Gonzalez AM, Buscaglia M, Ong M, Baird A. Distribution of basic fibroblast growth factor in the 18-day rat fetus: localization in the basement membranes of diverse tissues. *J Cell Biol* 1990; **110**: 753–765.
  31. Gomez-Pinilla F, Lee JW, Cotman CW. Distribution of basic fibroblast growth factor in the developing rat brain. *Neuroscience* 1994; **61**: 911–923.
  32. Eckenstein FP, Andersson C, Kuzis K, Woodward WR. Distribution of acidic and basic fibroblast growth factors in the mature, injured and developing rat nervous system. *Prog Brain Res* 1994; **103**: 55–64.
  33. Roach ES, Gomez MR, Northrup H. Tuberous sclerosis complex consensus conference: revised clinical diagnostic criteria. *J Child Neurol* 1998; **13**: 624–628.
  34. Mischel PS, Nguyen LP, Vinters HV. Cerebral cortical dysplasia associated with pediatric epilepsy. Review of neuropathologic features and proposal for a grading system. *J Neuropathol Exp Neurol* 1995; **54**: 137–153.
  35. Murphy M, Drago J, Bartlett PF. Fibroblast growth factor stimulates the proliferation and differentiation of neural precursor cells in vitro. *J Neurosci Res* 1990; **25**: 463–475.
  36. Van Der Wal EA, Gomez-Pinilla F, Cotman CW. Seizure-associated induction of basic fibroblast growth factor and its receptor in the rat brain. *Neuroscience* 1994; **60**: 311–323.
  37. Farrell MA, DeRosa MJ, Curran JG et al. Neuropathologic findings in cortical resections (including hemispherectomies) performed for the treatment of intractable childhood epilepsy. *Acta Neuropathol* 1992; **83**: 246–259.
  38. Cuevas P, Carceller F, Reimers D, Fu X, Gimenez-Gallego G. Immunohistochemical localization of basic fibroblast growth factor in choroid plexus of the rat. *Neurol Res* 1994; **16**: 310–312.
  39. Hayamizu TF, Chan PT, Johanson CE. FGF-2 immunoreactivity in adult rat ependyma and choroid plexus: responses to global forebrain ischemia and intraventricular FGF-2. *Neurol Res* 2001; **23**: 353–358.
  40. Frinchi M, Bonomo A, Trovato-Salinaro A et al. Fibroblast growth factor-2 and its receptor expression in proliferating precursor cells of the subventricular zone in the adult rat brain. *Neurosci Lett* 2008; **447**: 20–25.
  41. Mudo G, Belluardo N, Mauro A, Fuxe K. Acute intermittent nicotine treatment induces fibroblast growth factor-2 in the subventricular zone of the adult rat brain and enhances neuronal precursor cell proliferation. *Neuroscience* 2007; **145**: 470–483.
  42. Reid S, Ferretti P. Differential expression of fibroblast growth factor receptors in the developing murine choroid plexus. *Brain Res Dev Brain Res* 2003; **141**: 15–24.
  43. Wanaka A, Johnson EM Jr, Milbrandt J. Localization of FGF receptor mRNA in the adult rat central nervous system by in situ hybridization. *Neuron* 1990; **5**: 267–281.
  44. Yazaki N, Hosoi Y, Kawabata K et al. Differential expression patterns of mRNAs for members of the fibroblast growth factor receptor family, FGFR-1-FGFR-4, in rat brain. *J Neurosci Res* 1994; **37**: 445–452.
  45. Greenwood S, Swetloff A, Wade AM, Terasaki T, Ferretti P. Fgf2 is expressed in human and murine embryonic choroid plexus and affects choroid plexus epithelial cell behaviour. *Cerebrospinal Fluid Res* 2008; **5**: 20.
  46. Johanson CE, Szmydynger-Chodobska J, Chodobski A, Baird A, McMillan P, Stopa EG. Altered formation and bulk absorption of cerebrospinal fluid in FGF-2-induced hydrocephalus. *Am J Physiol* 1999; **277**: R263–R271.



# Endogenous catecholamine enhances the dysfunction of unfolded protein response and $\alpha$ -synuclein oligomerization in PC12 cells overexpressing human $\alpha$ -synuclein

Satoru Ito\*, Kazuhiro Nakaso, Keiko Imamura, Takao Takeshima, Kenji Nakashima

Department of Neurology, Institute of Neurological Sciences, Faculty of Medicine, Tottori University, Japan

## ARTICLE INFO

### Article history:

Received 7 July 2009

Received in revised form 29 September 2009

Accepted 6 October 2009

Available online 14 October 2009

### Keywords:

Parkinson's disease

$\alpha$ -Synuclein

Catecholamine

Quinone

Unfolded protein response

ER stress

## ABSTRACT

Parkinson's disease (PD) is a neurodegenerative disorder characterized by the selective loss of dopaminergic neurons and the presence of Lewy bodies.  $\alpha$ -Synuclein is a major component of Lewy bodies. Recently, many studies have focused on the interaction between  $\alpha$ -synuclein and catecholamine in the pathogenesis of PD. However, no detailed relationship between catecholamine and  $\alpha$ -synuclein cytotoxicity has been elucidated. Therefore, this study established PC12 cell lines which overexpress human  $\alpha$ -synuclein in a tetracycline-inducible manner. The overexpression of human  $\alpha$ -synuclein increased the number of apoptotic cells in a long-term culture. Moreover, human  $\alpha$ -synuclein expressing PC12 cells demonstrated an increased vulnerability to several stressors in a short culture period. Thapsigargin increased the SDS soluble oligomers of  $\alpha$ -synuclein associated with catecholamine-quinone. The unfolded protein response (UPR) study showed that thapsigargin increased eIF2 $\alpha$  phosphorylation and nuclear GADD153/CHOP induction under  $\alpha$ -synuclein overexpressed conditions. The activities of the ATF6 $\alpha$  and IRE1 $\alpha$  pathways decreased. These findings suggest that an overexpression of  $\alpha$ -synuclein partly inactivates the UPR.  $\alpha$ -Methyltyrosine inhibited the dysfunction of the UPR caused by an overexpression of human  $\alpha$ -synuclein. Therefore, these findings suggest that the coexistence of human  $\alpha$ -synuclein with catecholamine enhances the endoplasmic reticulum stress-related toxicity in PD pathogenesis.

© 2009 Elsevier Ireland Ltd and the Japan Neuroscience Society. All rights reserved.

## 1. Introduction

Parkinson's disease (PD) is the most common movement disorder and is pathologically characterized by selective dopaminergic neuronal death. Abundant evidence points to a causative role for the presynaptic protein  $\alpha$ -synuclein ( $\alpha$ -syn) in the pathogenesis of PD (Spillantini et al., 1998; Mizuno et al., 2008).  $\alpha$ -Syn is a major component of Lewy Bodies, cellular inclusion bodies that are the hallmark pathological feature of PD (Spillantini et al., 1998). The duplication and triplication of the  $\alpha$ -syn gene appears to be the cause of PD in rare cases of familial forms of PD (Singleton et al., 2003; Chartier-Harlin et al., 2004; Ibáñez et al., 2004). An overexpression of  $\alpha$ -syn leads to neurodegeneration in mouse, rat, fly, and nematode models of PD (Cooper et al., 2006; Auluck et al., 2002; Lo Bianco et al., 2002; Masliah et al., 2000; Cao et al., 2005).

These data show that storage of  $\alpha$ -syn may be involved in the pathogenesis of PD. Recent studies have shown that an overexpression of  $\alpha$ -syn can induce a mitochondrial deficit (Hsu et al., 2000), enhanced vulnerability to oxidative stress (Hsu et al., 2000; Prasad et al., 2004) and inhibition of endoplasmic reticulum (ER)-Golgi trafficking (Cooper et al., 2006; Sugeno et al., 2008). Moreover, other reports suggest that catecholamine (CA) such as dopamine (DA) and DOPA can stabilize the protofibrillar form of  $\alpha$ -syn (Conway et al., 2001) and endogenous DA enhances cell death associated with soluble  $\alpha$ -syn protein (Xu et al., 2002). However, the association of endogenous CA with  $\alpha$ -syn toxicity is still unclear.

Numerous studies of PD rely on drug models using 1-methyl-4-phenyl-pyridinium (MPP+), rotenone and 6-hydroxydopamine (6-OHDA). These agents cause a DA-neuronal death and PD-like phenotype in animal models. These agents also induce the unfolded protein response (UPR) in ER (Holtz and O'Malley, 2003; Ryu et al., 2002). Dysfunction of Parkin, a gene product responsible for autosomal recessive juvenile Parkinsonism (AR-JP), is linked to ER stress and the UPR (Imai et al., 2002, 2001). Accumulating genetic and molecular evidence suggests that defects in the ER contribute to the pathogenesis of PD.

**Abbreviations:** DMEM, Dulbecco's Modified Eagle Medium; SDS, sodium dodecyl sulfate.

\* Corresponding author at: 36-1, Nishicho, Yonago 683-8504, Japan.

Tel.: +81 859 38 6757; fax: +81 859 38 6759.

E-mail address: [s-itou@med.tottori-u.ac.jp](mailto:s-itou@med.tottori-u.ac.jp) (S. Ito).

Previous studies have demonstrated that UPR plays an important role in the pathogenesis of PD, and  $\alpha$ -syn relates to a part of UPR. However, it is unclear whether CA is involved in the  $\alpha$ -syn pathogenesis in response to ER stress. A human  $\alpha$ -syn overexpressing PC12 cell line that could be controlled in tetracycline dependent manner was established to investigate how ER stress and CA enhance the pathogenesis of human  $\alpha$ -syn.

## 2. Materials and methods

### 2.1. Chemicals and antibodies

Nerve growth factor (NGF) was purchased from Invitrogen (Carlsbad, CA, USA).  $\alpha$ -Methyltyrosine ( $\alpha$ -MT) was purchased from PFALTZ&BAUER (Waterbury, CT, USA). Thapsigargin and 2-melcaptoethanol were obtained from Wako (Osaka, Japan). Tunicamycin and rotenone were purchased from Sigma (Taufkirchen, Germany) and Calbiochem (Darmstadt, Germany), respectively. Mouse monoclonal antibody against human  $\alpha$ -syn and  $\beta$ -syn are purchased from BD Transduction laboratory (clone 42; Lexington, KY, USA). Anti-GRP78 (H-129), anti-ATF6 $\alpha$  (H-280), anti-IRE1 $\alpha$  (H-190) and anti-GADD153/CHOP (B-3) antibodies were purchased from Santa Cruz (CA, USA). Anti-eIF2 $\alpha$ , anti-phospho eIF2 $\alpha$  (Ser51) and anti- $\beta$ -actin antibodies were obtained from Cell Signaling Technology (Beverly, MA, USA). Mouse monoclonal antibody against phosphoserine was purchased from Sigma (PSR-45; St. Louis, MO, USA). Horseradish-peroxidase (HRP)-linked anti-goat IgG and FITC- or TR-conjugated secondary antibodies for immunohistochemistry were obtained from Santa Cruz. HRP-linked anti-mouse IgG and anti-rabbit IgG were from Amersham Biosciences (Buckinghamshire, UK).

### 2.2. Cloning of human $\alpha$ -syn and human $\beta$ -syn cDNA

Total RNA was purified from human brain tissue using a Total RNA purification kit (Promega, Tokyo, Japan), and reverse transcription was carried out by the usual method. cDNA of human  $\alpha$ -syn was amplified from brain cDNAs by PCR using the primers; 5'-ATGGATGTATTCATGAAAGGACTTCA-3' and 5'-TTAGGCTCAGGTTCTAGTCTTG-3'. cDNA of human  $\beta$ -synuclein ( $\beta$ -syn) was also amplified by PCR using the primers; 5'-AAGCTTAGGATGGACGTGTTTC-3' and 5'-ACTACGCCCTCTGGCTCATA-3'. The PCR products were subcloned into the TA cloning vector (pGEM easy, Promega), and the sequences were confirmed. Thereafter, the cDNA of human  $\alpha$ -syn or human  $\beta$ -syn was transferred into a pTRE2 vector (Clontech, Palo Alto, CA, USA) for this experiment.

### 2.3. Preparation of PC12 cell lines

PC12 cells containing the pTet-Off regulator plasmid (PC12 Tet-Off) were purchased from Clontech. The cells were maintained at 37 °C in 5% CO<sub>2</sub> in DMEM/F12 medium, supplemented with 5% fetal bovine serum, 10,000 unit/ml penicillin and 100 mg/ml streptomycin. The pTRE2 vector encoding the human wild-type (WT)  $\alpha$ -syn gene and pTK-hygromycin encoding a hygromycin resistant gene, were transfected into PC12 Tet-Off cells. The transfection of these vectors was carried out using TransFast<sup>TM</sup> Transfection Reagent (Promega) following the manufacturer's protocol. Clones were selected after hygromycin treatment (400  $\mu$ g/ml), and used to generate monoclonal cell lines. Screening of clones for  $\alpha$ -syn overexpression was performed by Western blotting. For this experiment, cells were cultured using doxycycline (Dox) containing medium, and lysates were collected 72 h after withdrawing Dox. The same procedure was carried out to establish the cell line of WT

$\beta$ -syn. In addition, PC12 cells were treated with NGF (5 ng/ml) in each process of the current study.

### 2.4. Detection of apoptotic cells

Hoechst 33342 (Sigma, St. Louis, MO, USA) was prepared as a 2 mM stock solution. A 1:500 dilution of the stock solution in PBS was prepared freshly. After washing with PBS, the cells were incubated with the diluted Hoechst dye solution for 2 h at room temperature. The number of apoptotic cells that had condensed or fragmented nuclei was counted using fluoroscopy.

### 2.5. Immunoblot analysis

NGF-treated PC12 cells were harvested from 6-well culture plates, and lysed in SDS-sample buffer (50 mM Tris-HCl, pH 6.8, 2% SDS, 10% glycerol, 1 mM PMSF, 2 mM EDTA). The nuclear fraction was prepared by centrifugation (15,000  $\times$  g, 10 min) after lysis in NP40 buffer (0.5% NP40, 1 mM Tris-HCl, pH 7.9, 500  $\mu$ M dithiothreitol, 100  $\mu$ M EDTA), followed by lysis in SDS-sample buffer. Aliquots (10–20  $\mu$ g) were separated by size on 7.5–12.5% acrylamide gels. Immunoblotting was performed as described previously (Yoshimoto et al., 2005).

### 2.6. Immunofluorescent staining

PC12 cells were fixed in 4% paraformaldehyde, washed with PBS, and incubated with ice-cold solution containing 95% ethyl alcohol and 1% acetic acid for 5 min. After washing with PBS twice, the cells were incubated with antibodies overnight at 4 °C. Next, the cells were washed with PBS twice, and incubated with FITC- or TR-conjugated secondary antibody at room temperature for 4 h. Thereafter, the cells were washed with PBS several times, and, finally, the slides were covered using a Vectashield (Vector Lab Inc., Burlingame, CA, USA).

### 2.7. Immunoprecipitation

The cells for immunoprecipitation were harvested and lysed in IP-lysis buffer (20 mM HEPES, pH 7.5, 150 mM NaCl, 1 mM EDTA, 10  $\mu$ g/ml leupeptin, 1 mM PMSF, 1% Triton X-100, and 0.1% SDS). The lysates were centrifuged at 12,000  $\times$  g for 10 min and the supernatant was transferred to another tube containing prepared Agarose – Protein A/G (Santa Cruz) – anti-IRE1 $\alpha$  antibody conjugate. The mixture was incubated at 4 °C for 12 h with gentle rotation, centrifuged at 5000  $\times$  g for 30 s, and the supernatant was discarded. The Protein A/G-agarose was washed five times with IP-lysis buffer and, finally, with IP-final washing buffer (20 mM HEPES, pH 7.5, 150 mM NaCl). The washed preparation was analyzed by Western blotting using an anti-phosphoserine antibody.

### 2.8. Statistical analysis.

Differences among treatment groups were tested by an analysis of variance (ANOVA) using the SPSS software system. Any differences in which the *P* value was less than 0.05 were considered to be statistically significant.

## 3. Results

### 3.1. Overexpression of human $\alpha$ -syn causes dopaminergic cell death

The PC12 cells expressed  $\alpha$ -syn in a Dox dose and time dependent manner (Fig. 1A and B). The overexpression of human  $\alpha$ -syn induced cell death significantly at 7 days (Fig. 1C).  $\alpha$ -MT, a

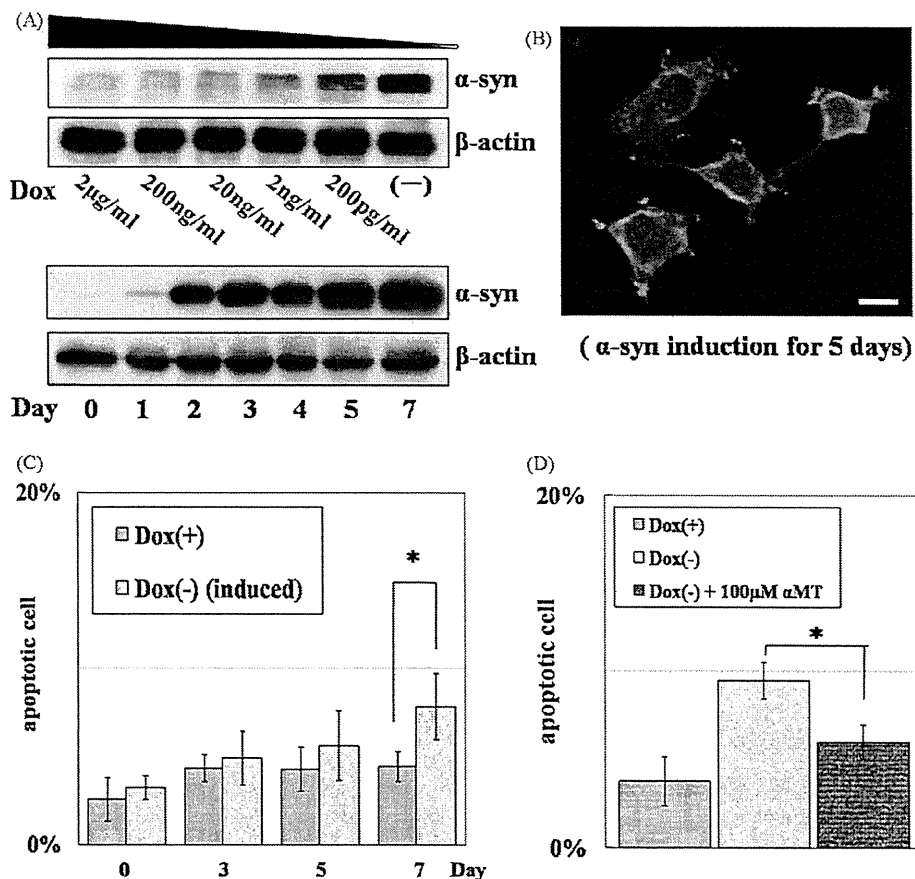


**Fig. 1.** Characterization of the PC12 cell line which expresses human  $\alpha$ -syn in a tetracycline dependent manner. (A) Neural differentiated PC12 cells were cultured and analyzed by Western blotting using anti- $\alpha$ -syn antibodies. The induced protein levels of  $\alpha$ -syn are observed in a dose dependent manner 3 days after  $\alpha$ -syn induction (upper lane). Withdrawal of Dox induces overexpression of  $\alpha$ -syn in a time dependent manner (lower lane). (B) There is a high level of  $\alpha$ -syn expression in PC12 cells cultured under induced conditions (Dox(-)) for 5 days. (C) The overexpression of human  $\alpha$ -syn induces cell death significantly at 7 days. (D) The number of apoptotic cells was decreased by the simultaneous administration of  $\alpha$ -MT (100  $\mu$ M) at 7 days. The scale bar represents 10  $\mu$ m.

specific inhibitor of tyrosine hydroxylase, was used to evaluate the association with CA. This reduced the number of apoptotic cells in response to  $\alpha$ -syn overexpression in 7 days (Fig. 1D). Consequently, endogenous CA metabolites were thus suggested to enhance the cytotoxicity of  $\alpha$ -syn.

### 3.2. Overexpression of human $\alpha$ -syn enhances cell vulnerability relating to CA

The overexpression of human  $\alpha$ -syn induced cell death was observed at 7 days after the induction of human  $\alpha$ -syn (Fig. 1C). Therefore, the cell vulnerability at 3 days after human  $\alpha$ -syn induction was investigated in the preclinical state of PD. An adequate amount of human  $\alpha$ -syn protein was observed at 3 days after human  $\alpha$ -syn induction, and  $\alpha$ -MT did not influence the expression level of human  $\alpha$ -syn (Fig. 2A). ER stressors, mitochondrial toxins and genotoxin were added into the cell medium and cultured for 20 h with or without 100  $\mu$ M  $\alpha$ -MT. The addition of 300 nM thapsigargin, 1  $\mu$ g/ml tunicamycin, 750  $\mu$ M MPP<sup>+</sup> and 1  $\mu$ M rotenone increased the number of apoptotic cells with the expression of human  $\alpha$ -syn (64.7%, 82.3%, 57.1%, 37.5% increase, respectively; Fig. 2B). However, the administration of 25  $\mu$ M etoposide showed no significant difference between the repressed and induced conditions. The inhibition of the CA metabolism by  $\alpha$ -MT revealed a decrease in the apoptotic cells in response to thapsigargin, tunicamycin, MPP<sup>+</sup> and rotenone

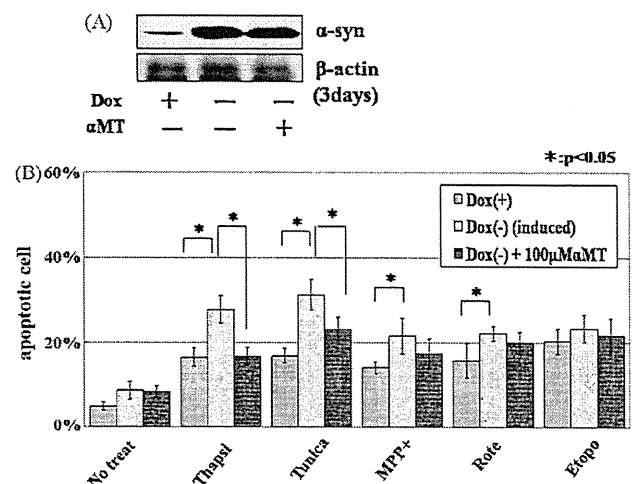


**Fig. 2.** Cell viability assay after induction of human  $\alpha$ -syn overexpression. Neural differentiated PC12 cells were incubated under repressed (Dox(+)) or induced (Dox(-)) conditions for 3 days. Another induced cell plate is treated with 100  $\mu$ M  $\alpha$ -MT. (A) A Western blot analysis shows the expression level of  $\alpha$ -syn. (B) After 3 days of  $\alpha$ -syn induction, neuronal PC12 cells were exposed to 300 nM thapsigargin (Thapsi), 1  $\mu$ g/ml tunicamycin (Tunica), 750  $\mu$ M MPP<sup>+</sup>, 1  $\mu$ M rotenone (Rote) and 25  $\mu$ M etoposide (Etopo) for 20 h. The number of apoptotic cells was counted under fluorescent microscopy. The histogram represents the ratio of apoptotic cells (apoptotic cells)/(total cells). Data are presented as the mean  $\pm$  SD. \* $P$  < 0.05.

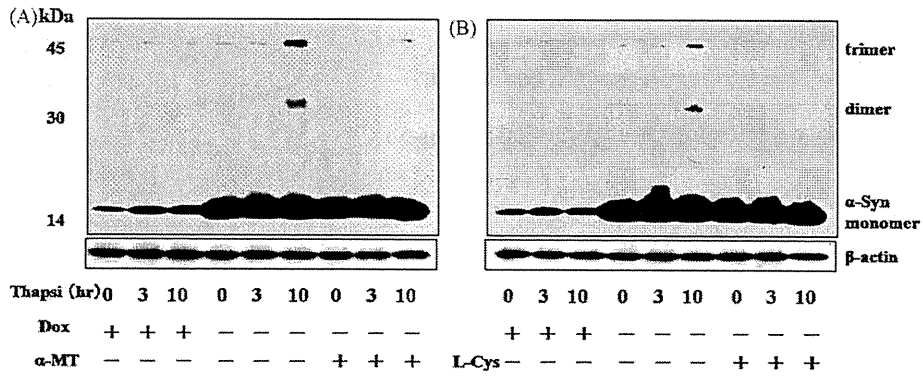


**Fig. 3.** An analysis of  $\alpha$ -syn oligomerization in response to thapsigargin. Neural differentiated cells were incubated for 3 days either under induced or repressed conditions. After 3 days of induction of  $\alpha$ -syn, cells are exposed to 300 nM thapsigargin for 0, 3 and 10 h. Cell lysates were analyzed by Western blotting with anti- $\alpha$ -syn antibody. A representative Western blot analysis reveals the increase of  $\alpha$ -syn oligomers 10 h after 300 nM thapsigargin exposure. Additional  $\alpha$ -MT (100  $\mu$ M) and L-cysteine (10  $\mu$ M) both decrease the oligomerization which is caused by thapsigargin.

(39.2%, 25.8%, 22.7%, 9.0% decrease, respectively). A significant decrease was observed in the number of apoptotic cells following  $\alpha$ -MT treatment in response to thapsigargin and tunicamycin exposure ( $<0.05$ ). These data suggest that  $\alpha$ -syn enhances cell vulnerability to stressors. In particular, endogenous CA metabolites lead to further enhancement of cell vulnerability to ER stressors.

**3.3. Thapsigargin enhanced  $\alpha$ -syn oligomerization in a presence of CA**

The kinetics of  $\alpha$ -syn following thapsigargin exposure were investigated. Thapsigargin increased oligomers of  $\alpha$ -syn in  $\alpha$ -syn overexpressed conditions. However, the inhibition of CA by  $\alpha$ -MT decreased the oligomerization of  $\alpha$ -syn (Fig. 3A). Moreover, L-cysteine, a scavenger of o-quinone, also decreased the oligomerization of  $\alpha$ -syn (Fig. 3B). These findings suggest that endogenous

CA and CA-related quinones are responsible for the observed increase in  $\alpha$ -syn oligomers.

**3.4. Overexpression of  $\alpha$ -syn suppresses UPR to thapsigargin**

The molecular behavior of the major three branches of the UPR, governed by the ER stress sensors IRE1 $\alpha$ , PERK-eIF2 $\alpha$ , and ATF6 $\alpha$ , respectively, were investigated to evaluate the influence of  $\alpha$ -syn on the ER. Protein levels of nuclear ATF6 $\alpha$  p50 (nATF6 $\alpha$  p50) were increased 1.5 h after thapsigargin exposure in  $\alpha$ -syn repressed conditions (136% relative increase). However, nATF6 $\alpha$  p50 showed a 62% relative increase under  $\alpha$ -syn induced conditions (Fig. 4A). IRE1 $\alpha$  was immunoprecipitated to determine whether there was any serine-phosphorylation of IRE1 $\alpha$  in order to identify the activation of the IRE1 $\alpha$ -related pathway. An increased level of phosphorylation of IRE1 $\alpha$  was observed at 1.5 h

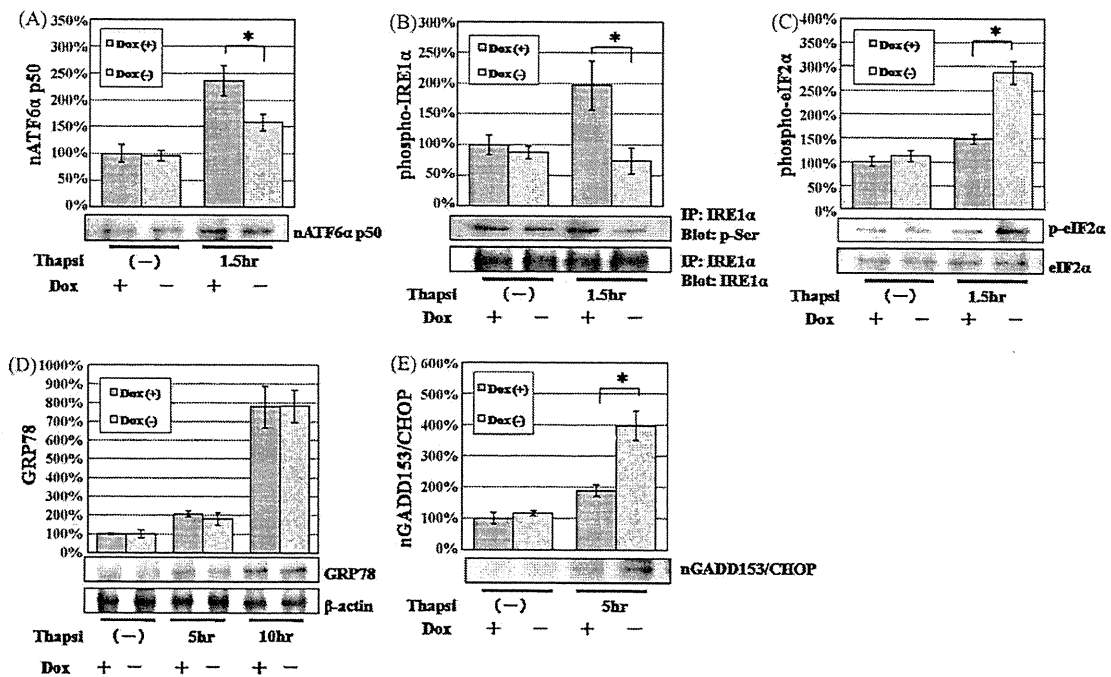


**Fig. 4.** An analysis of the unfolded protein response to thapsigargin. Differentiated PC12 cells were incubated for 3 days either under induced or repressed conditions. After 3 days, cells were exposed to 300 nM thapsigargin for 0, 1.5, 5 and 10 h. IRE1 $\alpha$  were immunoprecipitated and analyzed on a Western blot with phosphoserine antibody then with an antibody that recognizes total IRE1 $\alpha$ . Each histogram shows the semi-quantification data of the protein levels ( $N = 4$ ). The Western blot analysis reveals a decrease of nATF6 $\alpha$  p50 induction (A) and phosphorylation of IRE1 $\alpha$  (B) under  $\alpha$ -syn expressing conditions. No significant difference is observed in the induction of GRP78 (D). However, increases of both eIF2 $\alpha$  phosphorylation and nGADD153/CHOP induction are observed (C and E). Data are presented as the mean  $\pm$  SD. \* $P < 0.05$ .



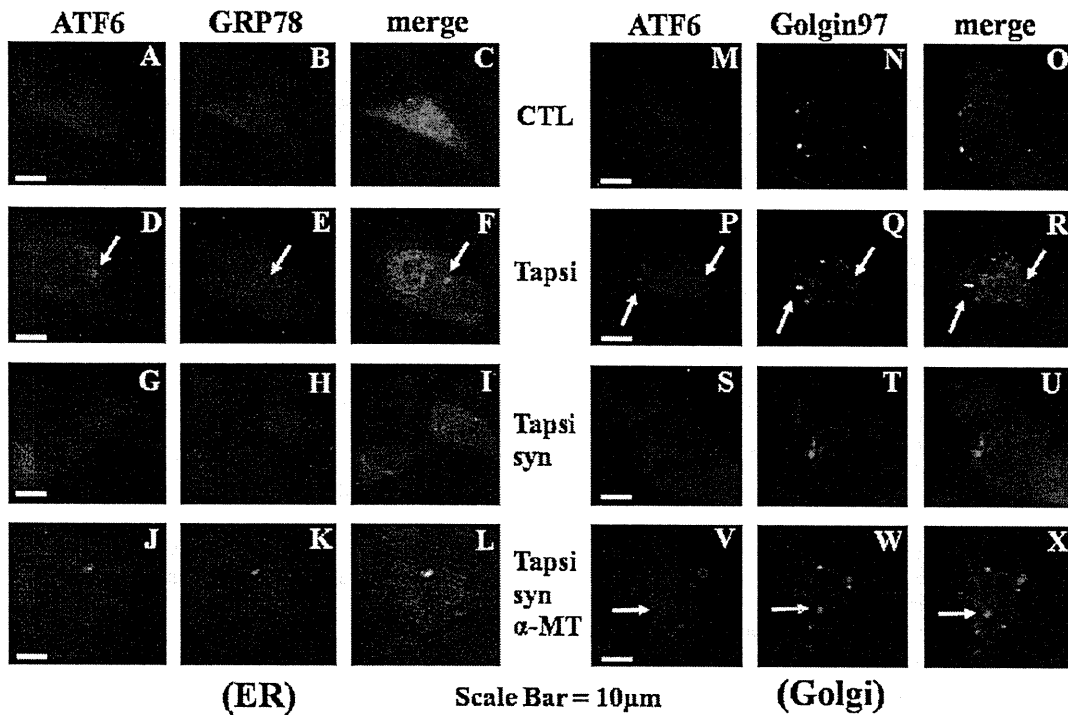


**Fig. 5.** Inhibition of ATF6 $\alpha$  trafficking to the Golgi apparatus by  $\alpha$ -syn overexpression. Neural differentiated cells were prepared in 8-well chamber slides (3 days induction). ATF6 $\alpha$  shows red fluorescence. Golgin97, a marker of Golgi apparatus, and GRP78, a marker of ER show green fluorescence. Under untreated conditions (CTL), ATF6 $\alpha$  is co-located with GRP78 (A–C), but not with Golgin97 (M–O). However, ATF6 $\alpha$  co-locating with Golgin97 is observed 3 h after exposure to 300 nM thapsigargin (P–R). Under  $\alpha$ -syn expressing conditions, the transfer of ATF6 $\alpha$  to Golgi apparatus is decreased (S–U). Additional  $\alpha$ -MT (100  $\mu$ M) increases ATF6 $\alpha$  co-locating with Golgin97 (V–X). The scale bar represents 10  $\mu$ m (For interpretation of the references to color in this figure legend, the reader is referred to the web version of the article).

after thapsigargin treatment (97% relative increase). However, the phosphorylation of IRE1 $\alpha$  was repressed by  $\alpha$ -syn overexpression (Fig. 4B). On the other hand, an increased level of phosphorylation of eIF2 $\alpha$  was observed at 1.5 h after thapsigargin treatment under  $\alpha$ -syn induced conditions (175% relative increase; Fig. 4C). Thapsigargin increased the expression level of GRP78, an ER chaperone that is vital for ER-stress induced UPR resolution (Fig. 4D). However, no significant

difference was observed between the repressed and induced conditions. Nuclear GADD153/CHOP (nGADD153/CHOP), a transcription factor that can induce apoptosis, showed a higher protein levels in  $\alpha$ -syn overexpressed conditions (282% relative increase) in comparison to repressed conditions (89% relative increase) 5 h after thapsigargin treatment (Fig. 4E). GRP78 and nGADD153/CHOP protein levels were measured under the same conditions using human  $\beta$ -syn overexpressing cells in order to investigate whether only an overexpression of protein influence UPR. Both GRP78 and nGADD153/CHOP did not show significant differences between the repressed and induced conditions (Supplementary data). Immunofluorescent staining suggested that the transfer of ATF6 $\alpha$  to the Golgi apparatus was inhibited by the overexpression of  $\alpha$ -syn (Fig. 5A–I, M–U).

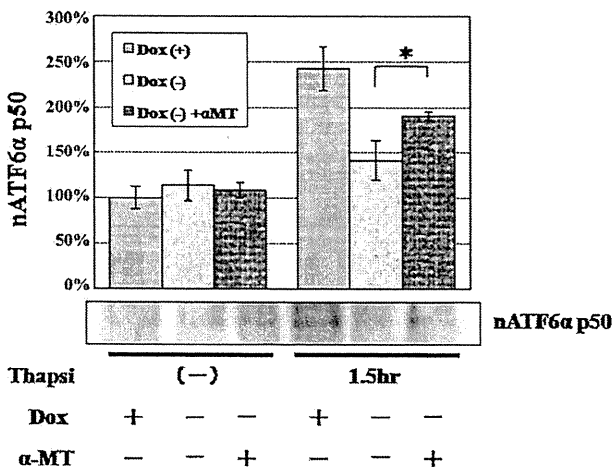


**Fig. 6.** Inhibition of endogenous CA prevents the reduction of nATF6 $\alpha$  p50. Differentiated PC12 cells were incubated for 3 days in either induced or repressed conditions. The cells are exposed to 300 nM thapsigargin for 1.5 h. The histogram shows the semi-quantification data of the nATF6 $\alpha$  p50 protein levels ( $N = 4$ ). Additional  $\alpha$ -MT (100  $\mu$ M) prevents the reduction of nATF6 $\alpha$  p50 caused by  $\alpha$ -syn expression. Data are presented as the mean  $\pm$  SD. \* $P < 0.05$ .

**3.5. Inhibition of CA metabolism rescues the ATF6 $\alpha$  inactivation caused by  $\alpha$ -syn overexpression**

Finally, the relationship between endogenous CA and the dysfunction of the ATF6 $\alpha$  pathway was investigated. Lower protein levels of nATF6 $\alpha$  p50 were observed in response to thapsigargin under  $\alpha$ -syn induced conditions (42% relative decrease) in comparison to repressed conditions (Fig. 6). However, the administration 100  $\mu$ M  $\alpha$ -MT reduced the inhibition of nATF6 $\alpha$  p50 induction under  $\alpha$ -syn overexpressed conditions (21% relative decrease). Moreover, immunofluorescent staining suggested that the inhibited transfer of ATF6 $\alpha$  to the Golgi apparatus was partially improved by  $\alpha$ -MT under  $\alpha$ -syn overexpressing conditions (Fig. 5J–L, V–X). These results suggest that endogenous CA enhances the impairment in ER–Golgi trafficking caused by the overexpression of human  $\alpha$ -syn.

#### 4. Discussion

Recent findings suggest that oligomers, rather than the fibrillar amyloid deposits of  $\alpha$ -syn, represent the principal toxic species in PD (Kayed et al., 2004). *In vitro* studies have also demonstrated that CA stabilizes the protofibrillar form of  $\alpha$ -syn, thus forming a CA- $\alpha$ -syn adduct (Conway et al., 2001). Therefore, the oligomerization of  $\alpha$ -syn may interact with CA in the pathogenesis of PD. On the other hand, environmental stressors have been used as a PD model both *in vitro* and in animals. Although dysfunctions of mitochondria, ER and ubiquitin-proteasome have been implicated in  $\alpha$ -syn pathogenesis (Mizuno et al., 2008), there is still insufficient evidence to determine whether CA is involved in these processes. A previous report demonstrated that L-DOPA and dopamine enhance the formation of aggregates under proteasome inhibition in PC12 cells (Yoshimoto et al., 2005). However, the amount of rat  $\alpha$ -syn in PC12 cells is so small that it is not easy to evaluate the formation of oligomers and aggregates without proteasome inhibition. Therefore, the current study employed the overexpression of human  $\alpha$ -syn in PC12 cells.

An increase in apoptotic cell death was observed over a 7-day incubation period, followed by an increase in the expression of human  $\alpha$ -syn. These cells were also vulnerable to ER stress and mitochondrial toxicities at an earlier incubation stage for 3 days (Figs. 1C and 2B). These findings indicate that an overexpression of human  $\alpha$ -syn is harmful in this cell line. Interestingly, WT  $\alpha$ -syn overexpressing models of PD often fail to reproduce the cardinal features of the disease (Giasson et al., 2002; Lee et al., 2002). On the other hand, only an overexpression of human WT  $\alpha$ -syn induces acute cell death in some neural-differentiated forms of human embryonic cells differentiated into neuroepithelial cells (Schneider et al., 2007). This suggests that the cell line in the current study is a suitable model to investigate the association between CA and the pathogenesis of PD.

Reduced apoptosis by  $\alpha$ -MT also suggests that CA enhances  $\alpha$ -syn toxicities (Figs. 1D and 2B). The neurotoxicity of CA-quinone formed by auto-oxidation of CA is associated with dopaminergic neuron-specific oxidative stress (Miyazaki et al., 2006). Although CA-quinone is a reactive metabolite that preferentially binds to reduced cysteine residues within polypeptides, it also binds covalently to  $\alpha$ -syn which has no cysteine residue (Conway et al., 2001; LaVoie et al., 2005). Since not only  $\alpha$ -MT but also L-cysteine inhibited an increase of  $\alpha$ -syn oligomers which were induced by thapsigargin administration (Fig. 3), CA-quinone formation might be involved in the pathogenesis of PD. The observed  $\alpha$ -syn oligomerization in response to thapsigargin was not associated with serine 129 phosphorylation of  $\alpha$ -syn (*data not shown*). Therefore, CA-quinone may directly interact with  $\alpha$ -syn protein and thereby cause a conformational change. Thapsigargin is an inhibitor of the  $\text{Ca}^{2+}$  pump in the ER membrane. Therefore, the disequilibrium of cytosolic  $\text{Ca}^{2+}$  probably causes oxidative stress, thus resulting in the enhancement of CA oxidation and the increase of toxic oligomers.

Since thapsigargin enhanced  $\alpha$ -syn cytotoxicity associated with CA, the UPR in ER was investigated. In mammals, three signaling pathways operate for the UPR, the IRE1-XBP1, PERK-eIF2 $\alpha$ , and ATF6 $\alpha$  pathways (Schröder and Kaufman, 2005). In the present study, thapsigargin activated eIF2 $\alpha$  phosphorylation and nGADD153/CHOP induction in  $\alpha$ -syn overexpressed conditions. However, the protein levels of ATF6 $\alpha$  p50 and IRE1 $\alpha$  phosphorylation decreased as a response to thapsigargin (Fig. 4). The inhibition of the CA metabolism therefore rescued the ATF6 $\alpha$  pathway dysfunction (Figs. 5 and 6). ATF6 $\alpha$  makes an initial response before the IRE1 $\alpha$  and PERK-eIF2 $\alpha$  pathways in mammals, and the signal transfer via ER-Golgi trafficking is unique to ATF6 $\alpha$  in the three signal branches of UPR (Chen et al., 2002). Therefore,

the impairment of the ATF6 $\alpha$  and IRE1 $\alpha$  pathways induced by CA-quinone might cause an earlier breakdown of UPR. The phosphorylation of eIF2 $\alpha$  has been reported to increase in human autopsy brain specimens obtained from PD patients (Hoozemans et al., 2007). These observations also support the current experimental findings.

#### Acknowledgments

This work was supported in part by Grants-in-Aid for Scientific Research from the Ministry of Education, Culture, Sports, Science and Technology of Japan (Nakaso), the Research Committee on Neurodegenerative Diseases, Ministry of Health, Labor and Welfare, Japan (Nakashima), and the Venture Business Laboratory, Tottori University (Ito).

#### Appendix A. Supplementary data

Supplementary data associated with this article can be found in the online version, at doi:10.1016/j.neures.2009.10.005.

#### References

- Auluck, P.K., Chan, H.Y., Trojanowski, J.Q., Lee, V.M., Bonini, N.M., 2002. Chaperone suppression of alpha-synuclein toxicity in a Drosophila model for Parkinson's disease. *Science* 295, 865–868.
- Schneider, Bernard, L., Seehus, Corey R., Capowski, Elizabeth E., Aebischer, Patrick, Zhang1, Su-Chun, Svendsen, Clive N., 2007. Over-expression of alpha-synuclein in human neural progenitors leads to specific changes in fate and differentiation. *Hum. Mol. Genet.* 16, 651–666.
- Cao, S., Gelwix, C.C., Caldwell, K.A., Caldwell, G.A., 2005. Torsin-mediated protection from cellular stress in the dopaminergic neurons of *Caenorhabditis elegans*. *J. Neurosci.* 25, 3801–3812.
- Chartier-Harlin, M.C., Kachergus, J., Roumier, C., Mouroux, V., Douay, X., Lincoln, S., Leveque, C., Larvor, L., Andrieux, J., Hulihan, M., Waucquier, N., Defebvre, L., Amouyel, P., Farrer, M., Destée, A., 2004. Alpha-synuclein locus duplication as a cause of familial Parkinson's disease. *Lancet* 364, 1167–1169.
- Chen, X., Shen, J., Prywes, R., 2002. The luminal domain of ATF6 senses endoplasmic reticulum (ER) stress and causes translocation of ATF6 from the ER to the Golgi. *J. Biol. Chem.* 277, 13045–13052.
- Conway, K.A., Rochet, J.C., Bieganski, R.M., Lansbury Jr., P.T., 2001. Kinetic stabilization of the alpha-synuclein protofibril by a dopamine-alpha-synuclein adduct. *Science* 294, 1346–1349.
- Cooper, A.A., Gitler, A.D., Cashikar, A., Haynes, C.M., Hill, K.J., Bhullar, B., Liu, K., Xu, K., Strathearn, K.E., Liu, F., Cao, S., Caldwell, K.A., Caldwell, G.A., Marsischky, G., Kolodner, R.D., Labaer, J., Rochet, J.C., Bonini, N.M., Lindquist, S., 2006.  $\alpha$ -synuclein blocks ER-golgi traffic and Rab1 rescues neuron loss in Parkinson's models. *Science* 21, 324–328.
- Giasson, B.I., Duda, J.E., Quinn, S.M., Zhang, B., Trojanowski, J.Q., Lee, V.M., 2002. Neuronal alpha-synucleinopathy with severe movement disorder in mice expressing A53T human alpha-synuclein. *Neuron* 34, 521–533.
- Holtz, W.A., O'Malley, K.L., 2003. Parkinsonian mimetics induce aspects of unfolded protein response in death of dopaminergic neurons. *J. Biol. Chem.* 278, 19367–19377.
- Hoozemans, J.J., van Haastert, E.S., Scheper, W., 2007. Activation of the unfolded protein response in Parkinson's disease. *Biochem. Biophys. Res. Commun.* 354, 707–711.
- Hsu, L.J., Sagara, Y., Arroyo, A., Rockenstein, E., Sisk, A., Mallory, M., Wong, J., Takenouchi, T., Hashimoto, M., Masliah, E., 2000. Alpha-synuclein promotes mitochondrial deficit and oxidative stress. *Am. J. Pathol.* 157, 401–410.
- Ibáñez, P., Bonnet, A.M., Débarges, B., Lohmann, E., Tison, F., Pollak, P., Agid, Y., Dürr, A., Brice, A., 2004. Causal relation between alpha-synuclein gene duplication and familial Parkinson's disease. *Lancet* 364, 1169–1171.
- Imai, Y., Soda, M., Inoue, H., Hattori, N., Mizuno, Y., Takahashi, R., 2001. An unfolded putative transmembrane polypeptide, which can lead to endoplasmic reticulum stress, is a substrate of Parkin. *Cell* 105, 891–902.
- Imai, Y., Soda, M., Hatakeyama, S., Akagi, T., Hashikawa, T., Nakayama, K.I., Takahashi, R., 2002. CHIP is associated with Parkin, a gene responsible for familial Parkinson's disease, and enhances its ubiquitin ligase activity. *Mol. Cell* 10, 55–67.
- Kayed, R., Sokolov, Y., Edmonds, B., McIntire, T.M., Milton, S.C., Hall, J.E., Glabe, C.G., 2004. Permeabilization of lipid bilayers is a common conformation-dependent activity of soluble amyloid oligomers in protein misfolding diseases. *J. Biol. Chem.* 279, 46363–46366.
- LaVoie, M.J., Ostaszewski, B.L., Weihofen, A., Schlossmacher, M.G., Selkoe, D.J., 2005. Dopamine covalently modifies and functionally inactivates parkin. *Nat. Med.* 11, 1159–1161.

- Lee, M.K., Stirling, W., Xu, Y., Xu, X., Qui, D., Mandir, A.S., Dawson, T.M., Copeland, N.G., Jenkins, N.A., Price, D.L., 2002. Human alpha-synuclein-harboring familial Parkinson's disease-linked Ala-53 → Thr mutation causes neurodegenerative disease with alpha-synuclein aggregation in transgenic mice. *Proc. Natl. Acad. Sci. U.S.A.* 99, 8968–8973.
- Lo Bianco, C., Ridet, J.L., Schneider, B.L., Deglon, N., Aebischer, P., 2002. Alpha-Synucleinopathy and selective dopaminergic neuron loss in a rat lentiviral-based model of Parkinson's disease. *Proc. Natl. Acad. Sci. U.S.A.* 99, 10813–10818.
- Maslah, E., Rockenstein, E., Veinbergs, I., Mallory, M., Hashimoto, M., Takeda, A., Sagara, Y., Sisk, A., Mucke, L., 2000. Dopaminergic loss and inclusion body formation in alpha-synuclein mice: implications for neurodegenerative disorders. *Science* 287, 1265–1269.
- Miyazaki, I., Asanuma, M., Diaz-Corrales, F.J., Fukuda, M., Kitaichi, K., Miyoshi, K., Ogawa, N., 2006. Methamphetamine-induced dopaminergic neurotoxicity is regulated by quinone-formation-related molecules. *FASEB J.* 20, 571–573.
- Mizuno, Y., Hattori, N., Kubo, S., Sato, S., Nishioka, K., Hatano, T., Tomiyama, H., Funayama, M., Machida, Y., Mochizuki, H., 2008. Progress in the pathogenesis and genetics of Parkinson's disease. *Philos. Trans. R. Soc. Lond. B. Biol. Sci.* 363, 2215–2227.
- Prasad, J.E., Kumar, B., Andreatta, C., Nahraini, P., Hanson, A.J., Yan, X.D., Prasad, K.N., 2004. Overexpression of alpha-synuclein decreased viability and enhanced sensitivity to prostaglandin E(2), hydrogen peroxide, and a nitric oxide donor in differentiated neuroblastoma cells. *J. Neurosci. Res.* 76, 415–422.
- Ryu, E.J., Harding, H.P., Angelastro, J.M., Vitolo, O.V., Ron, D., Greene, L.A., 2002. Endoplasmic reticulum stress and the unfolded protein response in cellular models of Parkinson's disease. *J. Neurosci.* 22, 10690–10698.
- Schröder, M., Kaufman, R.J., 2005. ER stress and the unfolded protein response. *Mutat. Res.* 569, 29–63.
- Singleton, A.B., Farrer, M., Johnson, J., Singleton, A., Hague, S., Kachergus, J., Hulihan, M., Peuralinna, T., Dutra, A., Nussbaum, R., Lincoln, S., Crawley, A., Hanson, M., Maraganore, D., Adler, C., Cookson, M.R., Muentner, M., Baptista, M., Miller, D., Blacato, J., Hardy, J., Gwinn-Hardy, K., 2003. Alpha-synuclein locus triplication causes Parkinson's disease. *Science* 302, 841.
- Spillantini, M.G., Crowther, R.A., Jakes, R., Hasegawa, M., Goedert, M., 1998.  $\alpha$ -Synuclein in filamentous inclusions of Lewy bodies from Parkinson's disease and dementia with Lewy bodies. *Proc. Natl. Acad. Sci. U.S.A.* 95, 6469–6473.
- Sugeno, N., Takeda, A., Hasegawa, T., Kobayashi, M., Kikuchi, A., Mori, F., Wakabayashi, K., Itoyama, Y., 2008. Serine 129 phosphorylation of  $\alpha$ -synuclein induces unfolded protein response-mediated cell death. *J. Biol. Chem.* 283, 23179–23188.
- Xu, J., Kao, S.Y., Lee, F.J., Song, W., Jin, L.W., Yankner, B.A., 2002. Dopamine-dependent neurotoxicity of alpha-synuclein: a mechanism for selective neurodegeneration in Parkinson disease. *Nat. Med.* 8, 600–606.
- Yoshimoto, Y., Nakaso, K., Nakashima, K., 2005. L-dopa and dopamine enhance the formation of aggregates under proteasome inhibition in PC12 cells. *FEBS Lett.* 579, 1197–1202.



ELSEVIER

Contents lists available at ScienceDirect

## Parkinsonism and Related Disorders

journal homepage: [www.elsevier.com/locate/parkreldis](http://www.elsevier.com/locate/parkreldis)

Short communication

Relationship between  $^{123}\text{I}$ -MIBG scintigrams and REM sleep behavior disorder in Parkinson's disease<sup>☆</sup>Takashi Nomura<sup>a,\*</sup>, Yuichi Inoue<sup>b,c</sup>, Birgit Högl<sup>d</sup>, Yusuke Uemura<sup>a</sup>, Michio Kitayama<sup>a</sup>, Takashi Abe<sup>b</sup>, Hidenao Miyoshi<sup>e</sup>, Kenji Nakashima<sup>a</sup><sup>a</sup> Division of Neurology, Department of Brain and Neurosciences, Faculty of Medicine, Tottori University, Japan<sup>b</sup> Japan Somnology Center, Neuropsychiatric Research Institute, Japan<sup>c</sup> Department of Somnology, Tokyo Medical University, Japan<sup>d</sup> Department of Neurology, Innsbruck Medical University, Austria<sup>e</sup> Department of Radiology, Faculty of Medicine, Tottori University, Japan

## ARTICLE INFO

## Article history:

Received 26 March 2010

Received in revised form

14 July 2010

Accepted 14 August 2010

## Keywords:

RBD symptoms

MIBG scintigrams

Parkinson's disease

RWA

## ABSTRACT

**Background:** Uptake of  $^{123}\text{I}$ -labeled meta-iodobenzylguanidine (MIBG) in myocardial scintigrams has been shown to be as low in patients with idiopathic RBD as in Parkinson's disease (PD) patients.

**Aim for study:** To clarify whether the existence of RBD accelerates autonomic dysfunction in PD, we investigated the association between MIBG scintigraphic findings and RBD measures among non-dementia PD patients.

**Subjects & methods:** We conducted clinical interviews to assess REM sleep behavior disorder (RBD) symptoms, and performed polysomnograms (PSG) recordings and MIBG scintigrams on 49 PD patients. The patients were divided into three groups (PD with clinical RBD, PD with subclinical RBD, and PD with normal REM sleep).

**Results:** PD patients with clinical RBD had reduced MIBG uptake as determined by heart-to-mediastinum ratios of the delayed image compared to those with subclinical RBD and those with normal REM sleep. Multiple linear regression analysis revealed that only the existence of RBD symptoms was significantly associated with reduced MIBG uptake among PD patients without dementia after adjusting for demographic and PD symptom-related variables.

**Conclusion:** PD patients with clinical RBD might suffer from a wider  $\alpha$ -synuclein pathology, including reduced cardiac sympathetic ganglia function as reflected by a lowered MIBG uptake.

Crown Copyright © 2010 Published by Elsevier Ltd. All rights reserved.

## 1. Introduction

REM sleep behavior disorder (RBD) is characterized by vigorous and injurious behaviors related to vivid, action-filled, and violent dreams in nocturnal REM sleep. RBD is diagnosed when a patient has both violent dream enactment behavior and REM sleep without atonia (RWA) on polysomnograms (PSG). RBD has been widely accepted as one of the important co-morbidities of PD [1] and has been proposed to be one of the risk factors for developing hallucinations [2] [3] in PD patients. Moreover, orthostatic abnormalities

were found to be more frequent in PD patients having RBD compared to those without these symptoms [3].

Cardiac uptake of  $^{123}\text{I}$ -labeled meta-iodobenzylguanidine (MIBG) on scintigrams is known to be reduced in PD patients [4]. Notably, reduced MIBG uptake on scintigrams in patients with idiopathic RBD is quite similar to that of PD patients [5]. However, it has not been determined whether reductions in MIBG uptake are lower in PD patients with RBD versus those without RBD. To clarify this issue, we investigated the association between MIBG scintigraphic findings and RBD measures among PD patients.

## 2. Methods

This study was approved by the ethics committees of Tottori University, and all patients gave informed consent to take part in it. Patients with PD who had been hospitalized in the Department of Neurology at the University Hospital from July 2004 to June 2008 were targeted for this study, and forty-nine PD patients agreed to participate. The mean follow-up period on the subject patients was  $6.3 \pm 5.1$  years. They had been receiving oral dopaminergic agents [levodopa dose equivalents

<sup>☆</sup> The review of this paper was entirely handled by an Associate Editor, Eng-King Tan.

\* Corresponding author. Division of Neurology, Department of Brain and Neurosciences, Faculty of Medicine, Tottori University, 36-1 Nishicho, Yonago 683-8504, Japan. Tel.: +81 859 38 6757; fax: +81 859 38 6759.

E-mail address: [ntnomura@med.tottori-u.ac.jp](mailto:ntnomura@med.tottori-u.ac.jp) (T. Nomura).